

**“Synthesis and Characterization of Iridium based
Metal Complexes and their applications in OLED”**

A Thesis Submitted

In partial fulfilment of the requirement

For the degree of

MASTER OF TECHNOLOGY

IN

MATERIALS AND METALLURGICAL ENGINEERING

By

Anil Kumar

Roll No. **600802002**



SCHOOL OF PHYSICS AND MATERIAL SCIENCE

THAPAR UNIVERSITY


PATIALA- 147004, INDIA


CERTIFICATE


This is to certify that the thesis entitled "Synthesis and Characterization of Iridium based Metal Complexes and their applications in OLED" submitted by Mr. Anil Kumar is in partial fulfilment for degree of master of technology in Materials and Metallurgical engineering of this University. This work has been done under our supervision. The work presented in this thesis is original to the best of our knowledge and has not been submitted to any other degree of this or any other University.

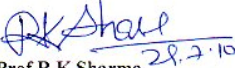
This work has been carried out from 4 January 2010 to 4 July 2010.

Supervisors


Dr. Ritu Srivastava
Scientist 'E1'
Centre for Organic Electronics
National Physical Laboratory
New Delhi – 110012


Dr.D.P.Singh
School of Physics and Material Science
Thapar University
Patiala-147004


Countersigned by:
Prof.O.P.Pandey
Head
School of Physics and Material Science
Thapar University
Patiala- 147004


Prof.R.K.Sharma
Dean, Academic Affair
Thapar University
Patiala-147004

DEDICATION

I would like to dedicate this dissertation to my parents, Mohinder Singh and Susheela Rani, my brother Sunil Kumar, my Jija Ji Santosh Kumar and my sister Jeenu for their inspiration, devotion, faith and support throughout this process.

ACKNOWLEDGEMENT

This thesis work is the final examination toward getting my master degree in Materials and Metallurgical Engineering at Thapar University, Patiala. The work has been carried out with the huge blessing of **God**.

I would like to express my deepest gratitude to **Dr. M.N.Kamalasanan** for providing me an opportunity to work in “**Centre for Organic Electronics**”, NPL. His astonishing language skills and his clear vision of scientific content help me in tremendous manner. Words can never express my deepest gratitude to my supervisors **Dr. Ritu Srivastava** and **Dr.D.P.Singh**, for their invaluable guidance and enthusiastic encouragement throughout my thesis work. Their excellent ideas, precious comments, strong confidence and farsighted outlook gave me confidence and enhanced my pleasure in the work. Without their genuine concern and unreserved support, I could not have finished my thesis work successfully.

Moreover, I am indebted to **Prof. O.P.Pandey**, Head, School of Physics and Material Science, Thapar University, Patiala for his support. Special acknowledgements are given to **Dr. R. C. Budhani (Director NPL)**, for permitting me to carrying out my thesis work at NPL.

Dr.A.K.Gupta, Dr.S.S.Bawa, Dr.Rajeev Chopra Head HRD group, NPL, for their support during the course of thesis work.

I pay thanks to Mr.Dharamveer Siani, from HRD group for his kind help.

I am deeply indebted to my teachers, Dr.K.K.Raina, Dr.N.K.Verma, Dr.Kulvir Singh, Dr.Sunil Kumar, Dr.Manoj Kumar, Dr.Puneet Sharma, Dr.Loveleen Brar and Dr.S.D.Tiwari. Their ideals and concepts have had a remarkable influence on my understanding in the field of Material Science and Engineering.

I would like to give my special thanks to Mr.Amit Kumar, Miss Punita, Miss Gayatri Chauhan, Mr.Arunandan Kumar, Miss Rakhi, Miss Omvati, Mr.Razi Ahmed, Miss Manisha Bajpayi , Miss Priyanka Tyagi, Mr.Anzar Gani, members of Centre for Organic Electronics for their kind support in my work. Mr.Amit Kumar helped me in all possible ways. Their timely discussions are very much appreciable.

I also would like to thanks my naughty friends Mr.N.P.Mishra, Mr. Pankaj Kumar, Mr.Ravinder Kumar, Mr.Mukesh Kumar, Mr.Aniruddha Dey, Mr.Arvind Choudhary, Mr.Ram, Mr.Gaurav, Mr.Aakash Katoch and Mr.Manjeet Singh.

Lastly I would like to thanks Uncle Ji, Mr. Raju and Mr. Hemant Kumar for their help in arranging laboratory materials during experiments.


Anil Kumar

ABSTRACT

Organic light-emitting devices (OLEDs) are emerging from the stage of research curiosity to the levels of important commercial applications. They are gaining acceptance as a promising flat panel display technology in this new millennium. However, OLEDs require further research and development, in particularly high performance emitting materials and electrodes, and novel device architectures since LCDs have a higher efficiency and longer operational lifetimes at the moment. The most important part of OLED devices is the electroluminescence layer, for which polymer and small molecular weight metal chelates can be used. The small molecule based metal chelates are the appropriate candidates as they are processed by conventional vacuum deposition techniques. Small molecule based Ir metal complexes can be used in OLED devices as electron and hole transport layer. It can also be used an emissive layer because of their wide spectral response in the visible region.

Two Iridium metal complexes [Ir(PBD)₂(Thenoyltrifluoroacetylacetonate)] and [Ir(PBD)₂(2,2,6,6-tetramethyl 3,5-heptadione)] have been synthesized and characterized by different characterization technique (FT-IR, NMR, UV-visible and photoluminescence spectroscopy). Excitation and emission properties of both the materials are extensively studied. The excitation spectra of [Ir(PBD)₂(Thenoyltrifluoroacetylacetonate)] shows absorption peak at 370 nm due to π - π^* transition from primary ligand and relatively weaker absorption peak at 433 nm due to metal to secondary ligand charge (¹MLCT) transition. The excitation spectra of [Ir(PBD)₂(2,2,6,6-tetramethyl 3,5-heptadione)] shows absorption peak at 362 nm due to π - π^* transition from primary ligand and relatively weaker absorption peak at 441 nm due to metal to secondary ligand charge (¹MLCT) transition. The range of 441-500 nm associated with both ³MLCT and ³ π - π^* transition. Both the complexes [Ir(PBD)₂(Thenoyltrifluoroacetylacetonate)] and [Ir(PBD)₂(2,2,6,6-tetramethyl 3,5-heptadione)] shows emission peaks at 559 nm and 549 nm respectively.

To investigate the electroluminescent properties of the complexes organic light emitting diode have been fabricated with the structure ITO/ α -NPD/(30nm)/Ir(PBD)₂(Thenoyltrifluoroacetylacetonate)(35nm)/BCP(6nm)/Alq₃(28nm)/LiF(1nm).

Electroluminescence spectra of the fabricated device show a broad electroluminescence peak at 565 nm. The current-voltage characteristic of the device shows turn on voltage about 9V. Therefore the present study provides a convenient way for colour tuning of the metal complexes by changing the secondary ligand.

CONTENTS

CHAPTER-1

INTRODUCTION

| | |
|---|----|
| 1.0 Introduction | 1 |
| 1.1 History of organic electroluminescence | 1 |
| 1.2 Types of luminescence | 3 |
| 1.2.1 Fluorescence | 3 |
| 1.2.2 Phosphorescence | 4 |
| 1.3 Photoluminescence and Frank-Condon-Shift | 5 |
| 1.4 Electroluminescence, charge injection, transportation and recombination | 6 |
| 1.5 Luminescence in organic materials | 7 |
| 1.6 Electroluminescence in organic materials | 8 |
| 1.7 Advantages of organic materials in electroluminescence processes | 8 |
| 1.8 Vapours-deposited small molecular OLED | 9 |
| 1.9 Polymeric OLED | 10 |
| 1.10 Flexible OLED | 10 |
| 1.11 Device structure of OLEDs and materials used | 11 |
| 1.11.1 Anode | 12 |

| | |
|--|----|
| 1.11.2 Hole transporting materials | 13 |
| 1.11.3 Electron transporting material | 15 |
| 1.11.4 Emissive material | 15 |
| 1.11.5 Cathode | 15 |
| 1.12 Types of OLEDs | 16 |
| 1.12.1 Passive and Active matrix OLEDs | 16 |
| 1.13 Techniques for OLED fabrication | 16 |
| 1.14 Working mechanisms of OLEDs | 17 |
| 1.15 Charge carrier transport | 18 |
| 1.16 Exciton formation | 19 |
| 1.17 Advantages and disadvantages of OLEDs | 20 |

CHAPTER-2

MOTIVATION AND SCOPE OF THE THESIS

| | |
|-------------------------|----|
| 2.1 Introduction | 22 |
| 2.2 Motivation | 23 |
| 2.3 Scope of the thesis | 24 |

CHAPTER-3

EXPERIMENTAL

Materials synthesis, their characterization and device fabrication

| | |
|---|----|
| 3.1 Synthesis | 26 |
| 3.1.1 Synthesis of Tetrakis[2,5-bis(4-methoxyphenyl)-1,3,4-oxadiazolyl-C ² ,N] (μ-dichloro)diiridium(III) | 26 |
| 3.1.1.1 Synthesis of mononuclear Ir(III) complexes using- Thenoyltrifluoroacetylacetone as secondary ligand | 27 |
| 3.1.1.2 Synthesis of mononuclear Ir(III) complexes 2, 2, 6, 6-tetramethyl 3,5-heptadione as secondary ligand | 28 |
| 3.2 Material characterization, device fabrication techniques: | 29 |
| 3.2.1 Materials characterization | 29 |
| 3.2.1.1 UV-Vis Spectrometer | 30 |
| 3.2.1.2 Photoluminescence spectroscopy | 31 |
| 3.2.1.3 Fourier Transforms Infra-Red spectroscopy | 32 |
| 3.2.1.4 Nuclear Magnetic Resonance spectroscopy | 34 |
| 3.2.2 Device fabrication technique | 35 |
| 3.2.2.1 Vacuum evaporation technique | 35 |
| 3.3 Device fabrication | 37 |
| 3.3.1 Ir(PBD) ₂ (Thenoyltrifluoro-acetone)] and Ir(PBD) ₂ (2,2,6,6- tetramethyl 3,5- heptadione) based organic light emitting diode | 37 |

CHAPTER 4

RESULTS AND DISCUSSION

| | |
|--|----|
| 4.1 Structural characterization | 39 |
| 4.1.1 Structural characterization of Ir(PBD) ₂ (Thenoyltrifluoroacetylacetonate) | 39 |
| 4.1.2 Structural characterization of Ir(PBD) ₂ (2,2,6,6-tetramethyl 3,5-heptadione) | 42 |
| 4.2 Optical characterization | 44 |
| 4.2.1 Optical characterization of Ir(PBD) ₂ (Thenoyltrifluoroacetylacetonate) | 44 |
| 4.2.2 Optical characterization of Ir(PBD) ₂ (2,2,6,6-tetramethyl 3,5-heptadione) | 45 |
| 4.3 Device characterization | 47 |
| 4.3.1 Device characterization of Ir(PBD) ₂ (Thenoyltrifluoroacetylacetonate) | 47 |

CHAPTER 5

CONCLUSION AND FUTURE SCOPE

| | |
|------------------|----|
| 5.1 Conclusion | 50 |
| 5.2 Future scope | 50 |
| References | |

LIST OF FIGURES

Figure 1.1: Energy transfer process

Figure 1.2: Frank Condon Shift in diatomic molecule

Figure 1.3: Basic steps involved in electroluminescence

Figure 1.4: Configuration of OLEDs

Figure 1.5(a): Basic structures of typical OLEDs

Figure 1.6: Chemical structure of typical HTMs

Figure 1.7: Schematic energy level diagram of a two-layer structure OLED

Figure 1.8: Diagram of organic electroluminescence process

Figure 3.1: Synthesis of Tetrakis[2,5-bis(4-methoxyphenyl)-

1-3,4-oxadiazolyl-C²,N](μ -dichloro)diiridium(III)

Figure 3.2: Synthesis of mononuclear Ir(III) complexes using

(Thenoyltrifluoro-acetone) as secondary ligand

Figure 3.3: Synthesis of mononuclear Ir(III) complexes using(2, 2, 6, 6-tetramethyl

3,5-heptadione)as secondary ligand

Figure 3.4: UV- Vis spectrometer

Figure 3.5: Working principle of UV-Vis spectrometry

Figure.3.6: Photoluminescence spectrophotometer

Figure 3.7: Schematic diagram of luminescence

Figure.3.8: FT-IR spectrophotometer

Figure 3.9: Arrangement of NMR spectrometer

Figure.3.10: Schematic diagram of the thermal vacuum evaporation process

Figure 3.11: Device structure of OLED

Figure 4.1: FTIR spectrum of $\text{Ir(PBD)}_2(\text{Thenoyltrifluoroacetylacetonate})$

Figure.4.2: (a) NMR (b) resolved NMR spectra of $\text{Ir(PBD)}_2(\text{Thenoyltrifluoroacetylacetonate})$ in CDCl_3

Figure 4.3: FTIR spectrum of $\text{Ir(PBD)}_2(2,2,6,6\text{-tetramethyl 3,5-heptadione})$

Figure.4.4 : (a)NMR(b) resolved NMR spectra of the $\text{Ir(PBD)}_2(2, 2, 6, 6\text{-tetramethyl 3,5-heptadione})$ in CDCl_3

Figure 4.5: UV-Vis spectrum of $\text{Ir(PBD)}_2(\text{Thenoyltrifluoroacetylacetonate})$

Figure 4.6: PL spectrum of $\text{Ir(PBD)}_2(\text{Thenoyltrifluoroacetylacetonate})$

Figure 4.7: UV-Vis spectrum of $\text{Ir(PBD)}_2(2,2,6,6\text{-tetramethyl 3,5-heptadione})$

Figure 4.8: PL spectrum of $\text{Ir(PBD)}_2(2,2,6,6\text{-tetramethyl 3,5-heptadione})$

Figure.4.9 : Electroluminescence spectra at different voltages

Figure.4.10: I-V characteristics of the device

LIST OF TABLES

Table1.1 Advantages and disadvantages of OLEDs

List of symbols and abbreviations

| | |
|-------|--|
| EL | Electroluminescence |
| °C | Degree Celsius |
| ITO | Indium-tin-oxide |
| PPV | poly-(para-phenylenevinylene) |
| PET | polyethylene terephthalate |
| TFEL | Thin Film Electroluminescent Displays |
| ETL | Electron Transporting Layer |
| HTL | Hole Transporting Layer |
| PBD | (2-(4-biphenyl)-5-(4-tertbutylphenyl)-[1,3,4]-oxadiazole |
| NPB | naphthylphenylbiphenyl diamine |
| CBP | 4, 4'-biscarbazolylbiphenyl |
| BCP | 2, 9-dimethyl-4,7-diphenyl-1, 10-phenanthroline |
| LUMO | Lowest Unoccupied Molecular Orbital |
| HOMO | Highest Occupied Molecular Orbital |
| E_F | Fermi Layer |
| TCL | Trapped Charge Limited |

| | |
|------------------|---|
| TDATA | 4,4' tris(<i>N,N</i> diphenylamino)triphenylamine |
| BPIBP | 4,4' bis(1,10phenanthroline[5,6]imidazole 2-yl)-biphenyl |
| Alq ₃ | tris(8-hydroxyquinoline) aluminium |

CHAPTER 1

INTRODUCTION

1.0 Introduction

Organic electroluminescent (EL) devices, also known as organic light emitting diodes (OLEDs), have some very attractive features that put it in a prominent position in the flat panel display market in this new millennium. Driving its future success is the continuing and accelerating development of both manufacturing process technology and exploration of new organic materials with excellent emissive properties. The organic EL technology, as an emerging technology, brings a new set of attributes to the display industry and has prompted scientists worldwide to further develop this new technology.

In general, the basic OLED structure consists of a stack of fluorescent organic layers sandwiched between a transparent conducting anode and metallic cathode [1,2]. When an appropriate bias is applied to the device, holes are injected from the anode and electrons from the cathode; some of the recombination events between the holes and electrons result in electroluminescence (EL).

1.1 History of organic electroluminescence

The first EL from an organic molecule, anthracene, was reported by Pope and his co-workers in 1963 [3]. They reported EL from a thick anthracene crystal (10 μ m-5mm), when a bias of several hundred volts was applied across it. The achievement did not stimulate much interest as the applied bias was very high. However, P. S. Vincent achieved bright blue EL from vacuum-deposited 0.6 μ m thick anthracene crystal films with an applied bias of less than 100V.

The breakthrough was achieved by Van Slyke in 1987, who made a bilayer structure by thermally evaporating the small molecular weight organic materials, N,N'-diphenyl-N,N'-bis(3-methylphenyl)1,1'-biphenyl-4,4'diamine(TPD) and tris(8-hydroxyquinoline) aluminum (Alq₃) to achieve a total thickness of ~100 nm. They achieved a very bright green emitting OLED with brightness higher than 1000 cd/m² and an external quantum

efficiency of ~1% when a low bias of 10V was applied across the structure. Following this achievement Adachi *et al* [4] succeeded in fabricating stable multilayer devices by inserting hole and electron transport layers between the two electrodes. In 1989, The laser-dye doped Alq₃ multilayer structure, in which the fluorescent efficiency was improved and the emission colour varied from the original green to the dopant emission color. Following the success of fabricating small molecular OLEDs, The first polymer LED (PLEDs) by spin coating a precursor polymer of the luminescent poly-(para-phenylene vinylene) (PPV) onto a indium tin oxide (ITO) coated glass. Compared to small molecular devices, polymer light emitting devices (PLEDs) have several potential advantages, e.g. fabrication by spin coating [5,6] or inkjet printing from solutions and subsequent thermal treatment.

Fluorescent emission of singlet excitons is the main mechanism of OLED light emission. As the probability of forming spin singlet states and spin triplet states are 25% and 75% respectively, the ideal maximum fluorescent yield is, therefore, limited to 25% by spin statistics. To overcome this theoretical limit Baldo *et al* [7] fabricated and demonstrated phosphorescent OLEDs, by doping phosphorescent molecules, where the EL is due to triplet emission, into a fluorescent host layer.

Electroluminescence refers to the phenomenon in which a solid (phosphor or semiconductor) emits light when an electric field is applied to it. Generally, EL can be classified into two types according to the active materials used in the device.

- Inorganic EL.
- Organic EL.

Organic EL is the emission of light upon electric excitation that leads to the radiative recombination of electrons and hole pairs injected into an organic semiconductor, in contrast to the inorganic EL which involves inorganic direct band gap semiconductors such as GaAs and ZnS. Two kinds of organic materials are utilized in organic EL.

- a. The first one is the small molecular organic compounds that can be sublimed under a vacuum for thin film deposition.
- b. The other one is the conjugated polymer that can be coated on different kinds of substrates from a solution.

On the contrary, inorganic EL has dominated the field of the EL sector of the flat panel display market in the past. However, some major deficiencies still remain in the inorganic EL despite decades of continuing development. Organic EL materials are gaining more and more attention owing to their versatility, rich blue photoluminescence, and high photoluminescence quantum yield [8]. The first report of EL in an organic material can be traced back to 1907 while the first success in the investigation of the organic electroluminescent phenomenon was achieved in 1963. The device was composed of a sandwiched layer of organic anthracene single crystal and two silver electrodes, and blue fluorescence was observed across the specimen under biased. A variety of studies of the mechanisms for transport and injection ensued, but the requirement of high operating voltages (50 – 1000 V) for injecting charges into the organic crystal in order to achieve a significant light output impractically low (typically < 0.1 %) EL efficiency of the device has seriously restricted its practical display applications. In 1982, Vincett *et al.* [9] used films of anthracene sublimed onto oxidized aluminium electrodes, with thermally evaporated semi-transparent top gold electrodes. The operating voltage was reduced to 30 V; however the quantum efficiency of their EL devices was only about 0.05 %. Although commercial interest in this subject has waned, it provided a general ground work for understanding organic EL.

1.2 Types of luminescence

There are two type of mechanism of luminescence called as fluorescence and phosphorescence, which are briefly explained in the subsequent subsections.

1.2.1 Fluorescence

Fluorescence is a process in which a luminophore absorbs a suitable energy photon to raise an electron from an occupied orbital to a higher energy vacant orbital, followed by the electron returning back to the original ground state energy level, and emitting a quantum of light with an energy corresponding to the energy difference between the excited state and ground state level, in such a way that the electron spin remains unchanged throughout the entire process. It means the molecule is either in its ground or excited singlet states all the time. This is a very fast process with luminescence lifetime of

the order of nanoseconds. Spin-allowed ($\Delta S=0$) transitions are called fluorescence. It quickly disappears when source of excitation (light or electric current) is removed.

1.2.2 Phosphorescence

Phosphorescence is a type of luminescence that results from the delayed recombination of triplet excitons. Emission of light from the triplets is delayed because it is forbidden to occur in the same molecule by the Pauli Exclusion Principle. It may occur only when the triplet excitons exchange its energy or excited electron with another molecule what is known as intersystem crossing. The process of intersystem crossing usually takes significant time to occur. Phosphorescence usually complies with the Stokes rule, in which emitted light is shifted to the lower energy region (red-shifted). However, anti-Stokes phosphorescence exists that is also known as delayed fluorescence. It happens when two triplets recombine to form a neutral molecule and a singlet exciton that possess higher energy. The latter recombines to emit a photon of higher energy (blue-shifted). Luminescence lifetime of phosphorescence is from some ten to microseconds up to milliseconds (**Figure 1.1**). Spin-forbidden transitions ($\Delta S=1$) is called phosphorescence. Internal conversion and other radiation less transfers of energy compete so successfully with phosphorescence that it is usually seen only at low temperatures or in highly viscous media.

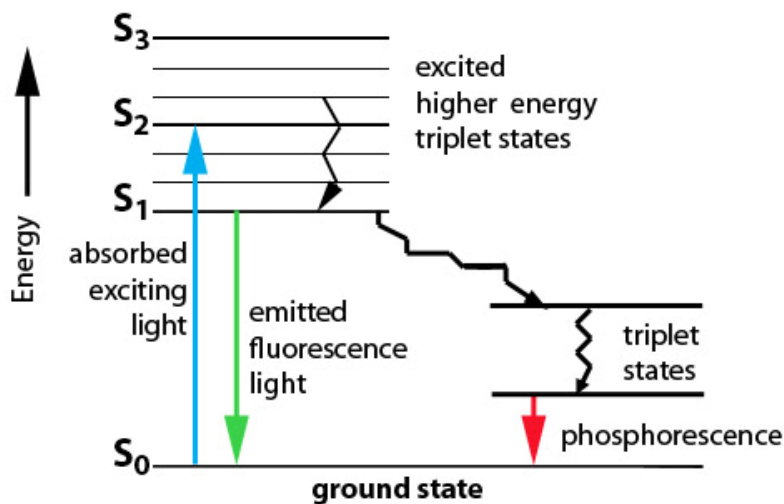


Figure 1.1: Energy transfer process.[56]

1.3 Photoluminescence and Frank-Condon-Shift

When an electron in the ground state absorbs a photon of energy E_A , it is promoted from the lowest ground state of the HOMO (S_0) to the corresponding vibronic sublevel of the LUMO (S_1) determined by the energy of the absorbed photon. After this, the electron relaxes non-radiatively down to the lowest vibrational sub-level of the LUMO ($\sim 10^{-13}$ sec). Because of the time needed for this process, the nuclei rearrange themselves. The electron then relaxes to the HOMO state by emission of a photon of energy E_B , because of the energy loss due to the vibronic levels, the emitted photon has a lower energy than the absorbed one. This energy shift between the absorbed and emitted photon is referred to as the Franck-Condon-Shift (**Figure 1.2**).

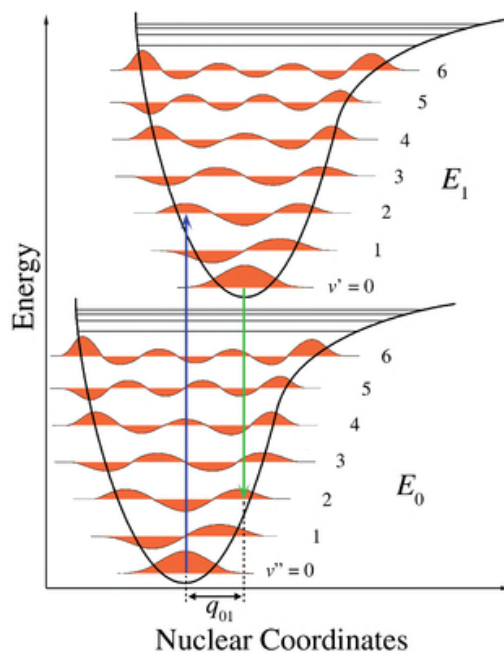


Figure1.2: Frank Condon Shift in diaomic molecule.[57]

1.4 Electroluminescence, charge injection, transportation and recombination.

Excitation by injection of electric charge is the most important mechanism in light emitting materials. If an electron is injected into an emitting material by means of an external electric field, it will have to occupy a LUMO state because all states below the HOMO are occupied. In this case, no emission can occur because the excited electron is unable to relax. Therefore, to obtain emission from the material, electrons and holes have to be injected at the same time. Both carriers then travel through the material in opposite direction under the influence of the external electric field. For fluorescent materials, the emission of a photon occurs when singlet excitons, formed by the coulombic interaction of electrons and holes with opposite spin states, radiatively decay to the molecular ground state. The region where this process occurs is referred to as the recombination zone (**Figure 1.3**). In the ideal case, all injected electrons recombine with a hole, i.e. the same number of electrons and holes has to be injected. The concept of “balanced injection” of carriers is an important aspect for the choice of materials. A significant disadvantage of fluorescent electroluminescence (EL) compared to photoluminescence (PL) is that emission can only occur from singlet excitons, limiting the electroluminescence efficiency (emitted photons per injected electron) in fluorescent materials to less than 25%. Theoretically, the PL efficiency can be unity because in this case all electron-hole pairs form singlet excitons.

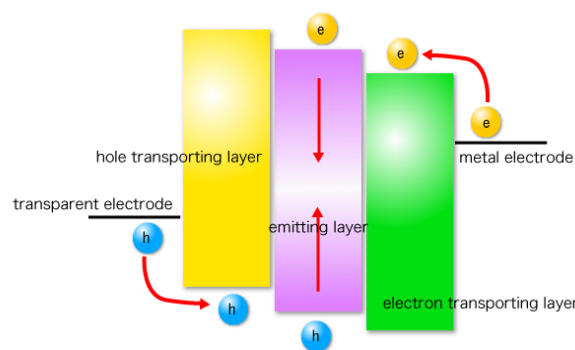


Figure 1.3: Basic steps involved in electroluminescence.[58]

Luminescent materials or light emitting materials are also known as phosphors. There are hundreds of phosphors, including some natural minerals and some biological compounds

and new phosphors are being discovered or synthesized in laboratories throughout the world due to their utilization in many devices of importance [10,11]. The scientific research on phosphors has a long history going back more than hundred years. From the 19th century to the early 20th century, Philip, E.A. Lenard and co-workers in Germany made active and extensive research on the phosphor and achieved impressive results [12]. They prepared various kinds of phosphors based upon alkaline earth chalcogenides, ZnS and various phosphors by using rare earth metals as activators also. Research on these materials has been supported by progress in advances in the understanding of the optical spectroscopy of solids especially that of transition metals ions and rare-earth ions.

1.5 Luminescence in organic materials

Organic materials refer to a base of the IV- group material carbon and with additional elements such as hydrogen (H), nitrogen (N), oxygen (O), phosphorus (P) and sulphur (S). Since organic materials are not referred as conducting materials because of the large band gap, a very high electrical field has to be applied. When applying an electrical field, the charge injections result in geometrical defects on the symmetric organic structure and exhibit a lower band gap. The charged carriers move along the structure and the attraction between the carrier's results in an exciton with a possibility to emit light as photons. The exciton is either in singlet or in triplet-state according to the Pauli's principle [13]. The exciton will form two new energy bands inside the band gap. Upon relaxation of the exciton, heat and photons will be emitted with an energy set by the energy difference between the energy bands that represent the exciton. The singlet-state is regarded as the light forming state, while triplet-state is not. In some special cases the triplet-state produces light as well. The backbone of the organic materials is made up of strongly localized bonds between the carbon atoms. The conductivity is enabled through conjugated π bonds. The length of the conjugation, i.e. the conjugation length, set certain characteristics of the molecule. The conjugation length defines the length where the electron is free to move. Naturally, small molecules tend to have short conjugation length, while longer conjugated molecules like polymers may have a longer. Longer conjugation length results in a smaller band gap. It is therefore easier to produce red light with conjugated polymers compared to small molecules, and consequently small molecules can more easily produce blue light. If the conjugation length of a molecule increases to infinity, the band gap is closely to zero, which could be compared to the conductivity for a

metal structure. This may be done by doping, i.e. introducing ions to the conjugated molecule, or by changing the side chains of the conjugated molecule.

1.6 Electroluminescence in organic materials

When an electrical field is applied, charge carriers are injected from the electrodes into the light emitting layer of organic materials respectively. The injection of the charged carriers, on to the organic chain, results through electron-phonon coupling in geometrical defects on the alternating structure, seen as polarons. The term electron-phonon coupling could be regarded as the “glue” between the bonding electrons of different atoms in the molecule [14]. Depending on the injected charged carrier, hole-and electron-polarons move along the emitting layer towards the opposite electrode and the emitting layer. The polarons exhibit two new states of energy between the HOMO and LUMO that lower the band gap E_g . The attractions of the polarons of positive and negative character perform a formation to an exciton-polaron [15]. The exciton-polaron has a spin and a property of singlet or triplet-state. The energy level of the exciton-polaron is below the conduction band and the released energy is emitted as photons. The states of the exciton-polaron have certain influence of the emission of light and quantum efficiency since the singlet states release its energy as an emission of photons. The amount of the emitted light could be reduced primarily by the triplet states. If the emission of light takes place at a too close distance to a metal cathode, the light could be reduced through quenching of exciton-polarons.

1.7 Advantages of organic materials in electroluminescence processes

The application of organic compounds as active components in electronic devices is very important. Since Van Slyke and Tang from Kodak prepared a thin film organic electroluminescent device in 1987, there has been special interest in the new technology of “cold” light emitting devices using organic phosphors [16]. Organic materials have some advantages over other non-organic luminescent materials, such as:

1. The organic materials are usually used as thin amorphous films, which can be processed easily over large area.

2. Amounts of organic materials are relatively small (100 nm thick) and large scale production (chemistry) is easier than for inorganic materials (growth processes of single crystals etc.).
3. They can be tuned chemically in order to adjust the separately band gap transport as well as solubility and several other structural properties.
4. The vast variety of possible chemical structures and functionalities of organic materials (polymers, oligomers, dendrimers, dyes, pigments, liquid crystals, etc.) favour an active research for alternative competitive materials with the desired properties.
5. The unique thing about organic material over the inorganic ones is that their emission is significantly red-shifted from their absorption bands, which is known as stokes shift [17].
6. Large amount of organic materials are known to have extremely high fluorescence quantum efficiencies in the visible spectrum, including the blue region, some approaching 100% efficiency.

1.8 Vapors-deposited small molecular organic light emitting diode

The development of organic EL reached an important milestone as a result of the effort of Tang and Vanslyk. When the material became ready for practical applications in the Kodak Research Laboratories, culminating in the 1987 demonstration of a double layer structure of a vacuum deposited small molecular film device as shown in **(Figure 1.4)**

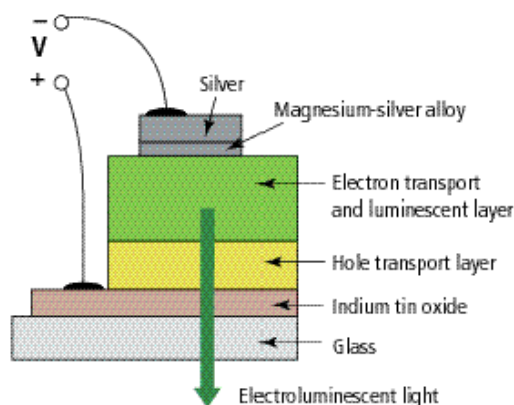


Figure 1.4: Configuration of OLEDs.[59]

Indium-tin-oxide (ITO) and a low work function alloy of magnesium and silver (Mg:Ag) were used as the anode and the electron-injecting cathode respectively. This device emits green light with much lower driving voltages (brightness greater than 1000 cd/m² below 10 V), while a higher quantum efficiency (1 %), high luminous efficiency (1.5 lm/W) and fairly good stability (100hours) was reported. Today, the device configuration: ITO/NPB/Alq₃/Mg:Ag is regarded as a prototypical structure of OLEDs or a so-called “standard device”. There are various nomenclatures of the OLEDs, which are based on utilized electroluminescent materials such as polymer light emitting diode employing polymer as luminescent material[18], flexible organic light emitting diode utilizes plastic substrate instead of glass substrate.

1.9 Polymeric organic light emitting diode

The advent of similar devices fabricated by Burroughs. of the Cambridge group in 1990 drew further attention to PLED. It was the first polymeric light-emitting device (PLED) with green light emission based on poly-(para-phenylenevinylene) (PPV) thin film. The discovery and development of its derivatives led to A. J. Heeger being awarded the Nobel Prize in Chemistry in 2000.

1.10 Flexible organic light emitting diode

Glass was used as the substrates in the OLEDs because glass has good inertness and strength. However, there are some disadvantages in using glass as it is brittle, inflexible and heavy. Another breakthrough occurred in 1992 when Gustafson *et al.* [19] fabricated the first fully flexible polymer-based OLED. Other than glass, polyethylene tetra phthalate (PET) sheets were utilized as the substrate. This is because PET sheets not only gave flexibility and toughness; it also lowered the weight of the devices. In 1996, The first flexible small molecule-based OLED using an ITO pre-coated transparent polyester as a substrate. It was reported that the performance of the flexible OLED (FOLED) was comparable to that deposited on glass substrates, and the FOLED did not deteriorate even under repeated bending. Since then, research in the use of organic materials as the active semiconductors in OLEDs has advanced rapidly, and enormous progress has been made in improving the color gamut, luminance efficiency and device reliability; this is due to the promise of the use of this technology in flat-panel full-color displays.

1.11 Device structure of organic light emitting diode and materials used.

An OLED consists of consecutive stacks of extremely thin organic layers (generally thinner than 0.2 μm in the total film thickness sandwiched between a low work function metal (and metal alloy) as cathode, and a transparent anode (e.g. ITO, AZO) [20]. Indium-tin-oxide (ITO) is a usual choice; it possesses a high work function of approximately 4.5 to 5.0 eV and has high transmittance and conductance. The top most layer is an electron-injecting cathode, typically made of a low-to-medium work function metal or metal alloy, such as Ca (2.9 eV), Mg:Ag (3.66 eV) or Al (4.3 eV). The organic layers, which comprise a hole-transporting layer (HTL) and an electron-emissive layer (EML), is called a basic two-layer device and this configuration was proposed by Kodak.

In this two-layer structure, the HTL is intentionally chosen to facilitate transport of holes while the other organic layer, i.e. ETL, is selected specifically for the transport of electrons [21]. The interface between the layers provides an efficient site for the recombination of the injected hole-electron pair, which results in electroluminescence. Reduced resistance is provided by the extremely thin organic EL medium. This permits a higher current density from a given level of electrical applied voltage. As light emission of OLEDs is directly related to the current density applied through the organic EL medium, the coupling effect of the thin organic layers increases the charge injection and transport efficiencies. This allows an acceptable light emission to be achieved with a low biased voltage. Such kinds of structures can be further modified into a three-layer structure, which was pioneered by researchers at Kyushu University [22] by sandwiching an additional luminescent layer, i.e. emissive layer (EML), between the ETL and HTL, as shown in **(Figure 1.5)**

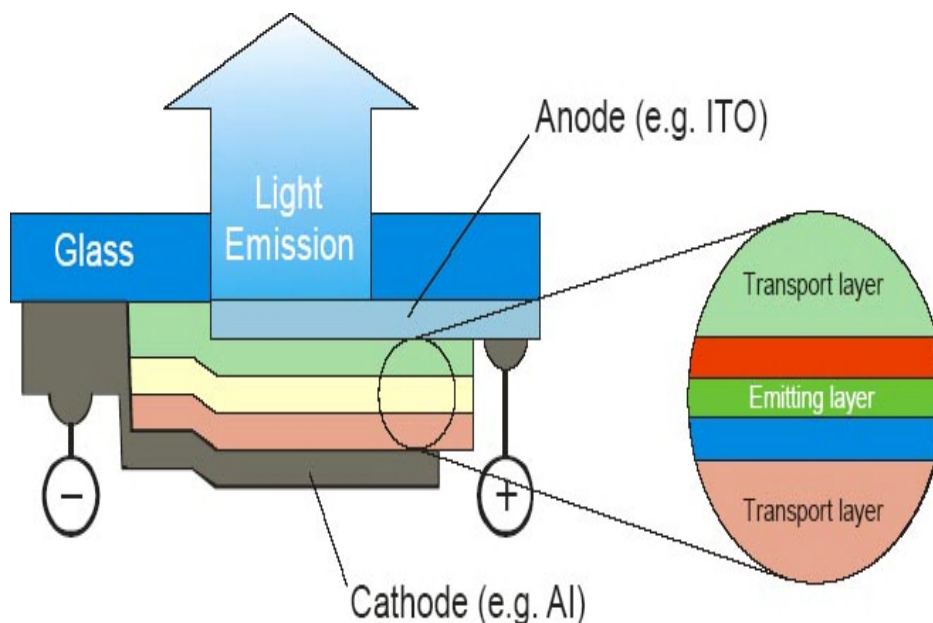


Figure 1.5: Basic structures of typical OLEDs.[60]

This EML provides the sites for hole-electron recombination and thus electroluminescence. In this structure, the functions of the individual organic layers are different and distinct, and can therefore be optimized independently. Hence, the luminescence or recombination layer can be chosen to have the desired EL colour with high luminescence efficiency. Similarly, the electron and hole transport layers can be optimized primarily for carrier transport property. In order to improve the device performance, it is important to understand the properties of materials which affect the performance of OLEDs. Organic materials can be tailored to serve specific functions. With appropriate chemical design composition, molecules can be modified to serve different functions in OLEDs. Generally, materials can be classified into hole transporting materials (HTM), light emitting materials (EM), and electron transporting materials (ETM), sandwiched between the anode and cathode according to the function of the materials in OLED [23].

1.11.1 Anode

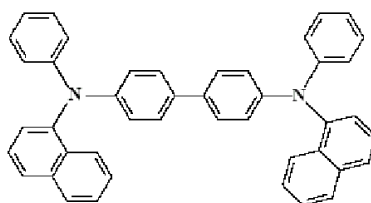
In a basic OLED structure, a transparent conductive oxide (TCO) layer is used as the anode. A common conducting metal oxide used as an anode is indium-tin-oxide (ITO). ITO is a good choice not only because it has a high work function of about 4.5 – 5.3 eV, but also because it is reasonably inert, highly electrically conductive can be easily

patterned, and optically transmission ($> 90\%$ transmission for visible light region), which enables light emission through the substrate. Preparation methods currently used include magnetron sputtering, spray pyrolysis, and chemical vapour deposition. In order to raise the work function of ITO, some commonly used surface treatments are adapted, these include acid treatment ultraviolet (UV)–ozone treatment and oxygen plasma treatment [24]. The employment of the surface treatment of ITO dramatically enhances hole injection, and device performance and reliability are improved significantly. Recently, Al-doped transparent conductive zinc oxide (AZO) films have been investigated as an alternative to ITO films [25]. AZO films with surface work functions between 3.7 and 4.4 eV were obtained by varying the sputtering conditions. In comparison to ITO, ZnO films are more stable in reducing ambient environment, more abundant, and less expensive. This makes AZO a competitive alternative for the anode which currently uses ITO.

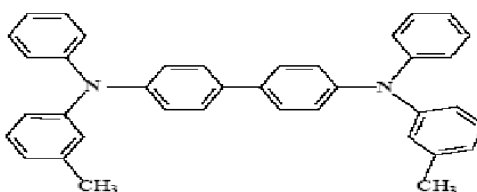
1.11.2 Hole transporting materials

The hole-transporting layer (HTL) can greatly improve the performance, i.e. the operational stability and EL efficiency, of OLED. It assists hole injection as a result of a better matching with the work function of the anode. It also facilitates hole (positive charge carriers) transports from the anode to the recombination zone, thus reducing the accumulation of charges at the anode and HTL interface. The material used in this layer is called hole transporting material (HTM). The choice of HTMs for organic electroluminescence (EL) applications is mainly focused on materials with a high thermal stability, high glass transition temperature (T_g), small energy barrier at the interface of anode/HTL (i.e low ionization potential, I_p) and good film forming properties [26]. Aromatic amines are commonly used as HTL materials. Within this amine class, one of the most widely used HTM material is small molecule OLED is a-naphthylphenylbiphenyl diamine (NPB). NPB was first demonstrated by Vanslyke and Tang and is a benzidine derivative with naphthyl substituent. The bulky naphthyl moiety in the molecule provides a more rigid structure and thus substantially high T_g of $98\text{ }^\circ\text{C}$. It is considerably higher than that of another well known HTM of N, N'-diphenyl-N, N'-bis (3-methyl phenyl) (1,1'-biphenyl)-4,4'-diamine(TPD) ($T_g = 60\text{ }^\circ\text{C}$). Another commonly used HTM is copper phthalocyanine (CuPc) which is combined with NPB to construct double HTLs. Actually, CuPc inhibits hole injection and is detrimental to the device characteristics [27]. The most appealing advantages of CuPc is its ability to planarize the irregularities present at the ITO

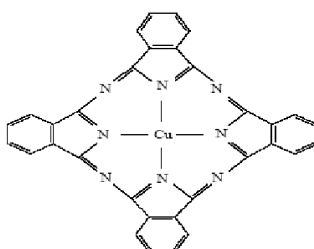
surface, and its superior film uniformity. Forsythe reported that NPB organic molecules grow in island-like modes on a pristine ITO surface using atomic force microscopy. However, they grow layer by layer with the presence of CuPc. This excellent uniformity apparently improves film adhesion, and is crucial to the operational stability of the devices. The chemical structures of NPB, TPD and CuPc are shown in **(Figure 1.6)**



NPB



TPD



CuPc

Figure 1.6: Chemical structure of typical HTMs

1.11.3 Electron transporting material

An electron-transport layer is introduced to reduce the electron injection barrier of the cathode and transport electrons from the cathode to recombine with holes [28]. An effective ETM has a low lowest unoccupied molecular orbital (LUMO) and a high ionization potential (Ip). Metal chelates and in particular Alq₃ are of most prevalent ETMs. Alq₃ is the most commonly used ETM due to its relatively good overall performance. It gives green emission at around 530 nm in the photoluminescence (PL) spectrum. In addition, it has a large electron affinity (E_A) of 3.1 eV, which minimizes the electron injection barrier from the cathode. It has also an unusually good thermal and morphological stability because of its high molecular symmetry.

1.11.4 Emissive material

Holes and electrons are recombined in the EML so as to prevent quenching of the excitons near the metallic cathode surface. Light will be emitted upon hole-electron recombination and the emissive wavelength depends on the band gap of the EML material. Alq₃ can be utilized as the EML because it is a good material for transporting electrons. Also, it is capable of emitting with a very good operation stability [29]. It has been reported that the emissive material has an electron transporting nature since the recombination of the charge carriers takes place in the narrow Alq₃ layer which is far away from the metal cathode.

1.11.5 Cathode

Metal cathodes with a low work function such as Mg, Ca, Li, etc. are used to reduce the barrier height for electron injection. Organics tend to have low electron affinities, so lower work function metals tend to inject electrons much better. For metals having a low work function, the barrier height between the Fermi-level of the cathode and the LUMO will be minimized. Alkali, alkaline and rare-earth (lanthanides) metals are ideally suited although they are mostly reactive and highly susceptible to atmospheric oxidation and corrosion. Accordingly, either covering with or incorporating of stable metals, such as aluminium (Al) or silver (Ag), is employed to provide some degree of stabilization. The typical choice as the cathode in small-molecular OLEDs is Mg-Ag alloy.

Magnesium (Mg) is a relatively stable metal with a work function of 3.6 eV, which is

sufficiently low to render it suitable as an electron injection electrode. The small amount of Ag is added to improve the sticking coefficient of Mg and hence assists Mg adhesion and to increase the conductivity of the electrode. Furthermore, the small amount of Ag helps to retard the degradation process, as Mg is very active and susceptible to atmospheric oxidation and corrosion. The development of a bilayer cathode with the structure of LiF/Al, first demonstrated by Wang *et al.* [30] marked another milestone. The utilization of the LiF/Al resulted in a substantial reduction in driving voltage and an increase in luminous efficiency. Thereafter, numerous researches using different insulating materials instead of LiF have been reported including CsF, NaCl, Al₂O₃ and have shown similar beneficial effects. Studies on the underlying working principle have been carried out, and it was revealed that the enhancement of electron injection is attributed to the liberation of low work function alkali or alkaline earth metal atoms.

1.12 Types of organic light emitting diode

There are several ways to classify OLEDs typically.

1.12.1 Passive and Active matrix organic light emitting diode

PMOLEDs are easy to make, but they consume more power than other types of OLED, mainly due to the power needed for the external circuitry. PMOLEDs are most efficient for text and icons and are best suited for small screens (2- to 3-inch diagonal) such as those you find in cell phones, PDAs and MP3 players. AMOLEDs consume less power than PMOLEDs because the TFT array requires less power than external circuitry, so they are efficient for large displays. AMOLEDs also have faster refresh rates suitable for video. The best uses for AMOLEDs are computer monitors, large-screen TVs and electronic signs or billboards.

1.13 Techniques for organic light emitting diode fabrication

Techniques for the Organic materials can be classified in the following two broad categories.

- Evaporation
- Wet processing

Evaporation techniques which are suitable for small molecules are:

- a. Sputtering
- b. E – beam evaporation
- c. Vapour deposition

Sputtering and electron–beam evaporation are used for high temperature material. Organic materials have low glass transition temperature so these techniques can damage the organic layers. Sputtering is one of the most versatile methods used for the deposition of transparent conductors when device-quality films are required. Compared with other deposition techniques, the sputtering process produces films with a higher quality and better-controlled composition, provides films with a higher adhesive strength and homogeneity and permits better control of film thickness.

Small molecular compounds and metal electrode can be deposited under a vacuum (10^{-6} Torr or better) by thermal evaporation. Solid materials will vaporize when heated to a sufficiently high temperature. The condensation of the vapour onto a relatively cool substrate yields a thin solid film. The deposition rate and thickness of the film can be controlled and measured by many well-developed techniques such as a quartz-crystal monitor. It is a sensitive microbalance that measures the actual changes in the resonant frequency of the quartz-crystal oscillator when the mass loading on the crystal changes. A quartz-crystal monitor can check and control both the deposition rates and the total thickness of the final films. Using properly matched shadow masks for depositing RGB emitting materials, segmented-color or full-color displays can be easily achieved. One of the most salient advantages of thermal vacuum evaporation is that the thickness of each layer and the doping of dyes can be controlled systematically and easily fabricated in a single deposition procedure [31].

1.14 Working mechanisms of organic light emitting diode

An OLED works on the principle of electroluminescence [32]. Injection of holes occurs from the anode into the HTL when a positive electrical potential is applied to the anode. On the other hand, electrons are injected from the cathode into the ETL when a negative electrical potential is applied to the cathode of the device. The highest occupied molecular orbital (HOMO) of the HTL is slightly above that of the ETL, so holes can easily enter

into the ETL (**Figure 1.7**). However, electrons are confined in the ETL region because the lowest unoccupied molecular orbital (LUMO) of the ETL is significantly below that of HTL. Also, the hetero junction design of the OLED is to facilitate the hole injection from the HTL into the ETL and to block the electron injection in the opposite direction. This enhances the probability of exciton formation and recombination near the interfacial region. The mobility of holes in ETL is slow; hence the recombination between holes and electrons is enhanced. Since excitons are unstable, the excited energy is released in a form of electromagnetic wave (e.g. visible light) with a wavelength corresponding to the energy difference between the ground and the excited state. The emitted light is partially reflected by the metal cathode, and most of it is passed through the transparent anode and substrate for viewing by an observer. Different emissive materials can give different colors of light.

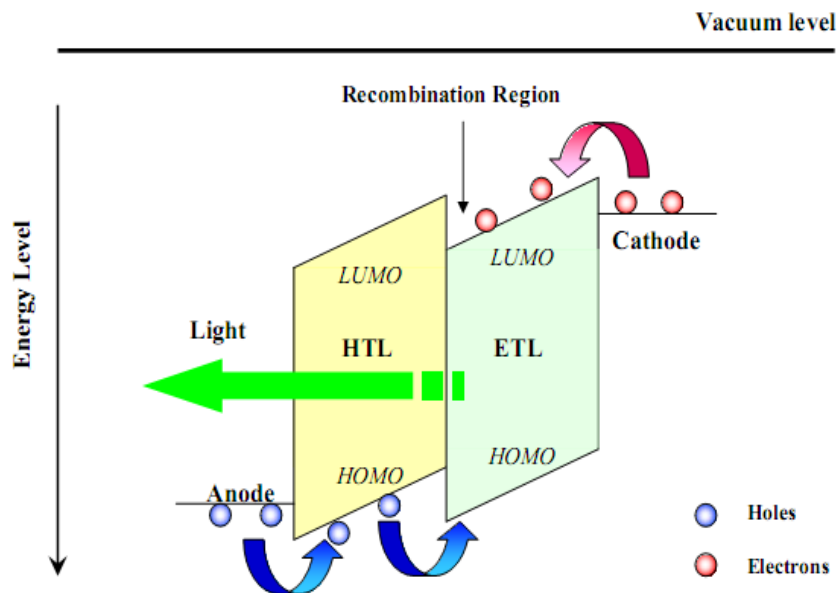


Figure 1.7: Schematic energy level diagram of a two-layer structure OLED.[61]

1.15 Charge carrier transport

The charge injections from both the cathode and anode electrodes to the organic layer as well as the charge transportation are important factors to reduce the operating voltage and increase the luminance efficiency of OLEDs. Usually, the electron mobility in electron-transport materials such as Alq₃ is one or two orders of magnitude lower than the holes mobility in hole-transport materials such as NPB. The hole mobility of NPB is in the range of 10^{-3} cm²/Vs which is two or three orders of magnitude higher than the electron

mobility in Alq₃. In this case, the limiting factor for low voltage operation and device power efficiency is the electron current from the cathode to the luminescent organic layer.

In addition, it was found that the current showed a power law dependence on the voltage. Actually the current-voltage characteristic is related to the injection of carriers into the organic thin film in which a large density of traps is distributed in energy beneath the LUMO. This concept revealed that trapped-charge-limited (TCL) currents dominate the transport in OLEDs at a high injection current. For instance, if the I-V characteristics of Alq₃ based OLEDs are analyzed over a wide range of temperatures, an exponential distribution of traps is revealed with a characteristic energy of 0.15 eV below the LUMO of Alq₃. For this reason, the intrinsic distribution of traps limits the flow of the current. In order to increase the luminescence efficiency, the injection and mobility of both charge carriers (electrons and holes) should be increased.

1.16 Exciton formation

After the charge injection from both electrodes to the organic layers, the holes and electrons recombine to form excitons and produce light upon radiative decay. There are two kinds of excitons: singlet and triplet. The radiative decay from the singlet state (generally in ns order) is relatively faster than the decay of the triplet state (generally in μ s). The former case is called fluorescence [33]. According to the conservation of spin, the decay from the triplet state to singlet ground state is not allowed and often non-radiative. However, in the presence of heavy atoms, spin-orbital coupling and exciton relaxation can lead to radiative decay from the triplet to singlet state. This case is called phosphorescence. Since different decay mechanisms possess different decay lifetimes, the decay lifetime is an important feature distinguishes fluorescence and phosphorescence. 75 % of the excitons formed by electron-hole recombination are into triplet states, and the remaining 25 % of excitons are in the singlet states which follow the spin statistics [34]. Fluorescence and phosphorescence are distinguished by the change of the spin quantum number (ΔS) between the initial and final states from the quantum physics aspect. When $\Delta S = 0$ (anti-symmetric molecular excitation), the emission process is defined as fluorescence and spinning is allowed in its transition. When $\Delta S \neq 0$ (spin-symmetric molecular excitation), the emission process is defined as phosphorescence. In the presence of spin-orbital coupling, triple emission is partially allowed [35]. In fluorescence

materials, only singlet excitons can undergo radiative decay to give light emission. As a result, the efficiency of fluorescence-based OLEDs normally has an upper limit of 25 %. For organic materials consisting of elements of a high atomic number such as iridium (Ir), platinum (Pt) and rhodium (Rh), spin-orbital coupling is drastically enhanced. This leads to considerable singlet-triplet state mixing, and so the remaining 75 % triplet decay can also promote radiative decay and lead to phosphorescence [36]. (Figure 1.8) summarizes the processes responsible for electroluminescence described above, including charge carrier injection from the electrodes, the capture of oppositely charged carriers (recombination), and the radiative decay of the excitons produced, which is crucial to device operation.

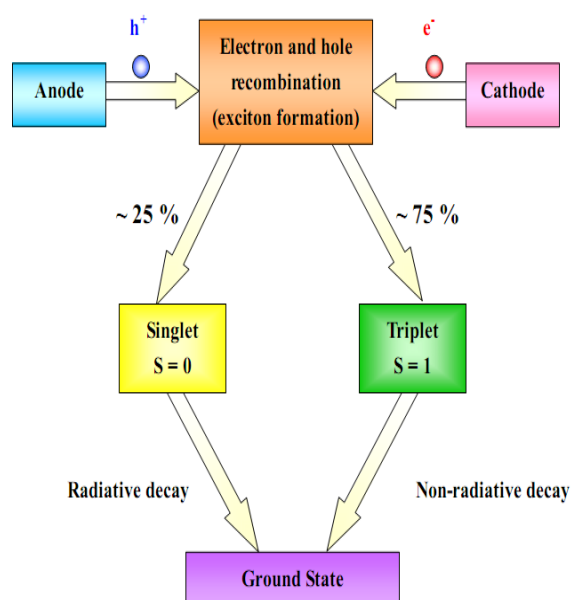


Figure 1.8: Diagram of organic electroluminescence process.[62]

1.17 Advantages and disadvantages of organic light emitting diode

OLEDs are already commercialized and they are making ways to the display markets. Currently OLEDs are used in low information displays with limited size such as mobile phones, PDAs, MP3 players, digital cameras and some laptop cameras. The driving force behind this success is some advantages that the OLEDs enjoy.

Table 1.1: Advantages and Disadvantages of the OLEDs

| S. No | Advantages | Disadvantages |
|--------------|--|--|
| 1. | Robust Design | Highly susceptible to degradation by oxygen and water molecules. |
| 2. | 170° images viewing angle | Less lifetime |
| 3. | Extra ordinary brightness | Low glass transition temperature |
| 4. | Clear distinct images | Low mobility due to amorphous nature of the organic molecules |
| 5 | Applicability in wide temperature operating range(40-85°C) | |

CHAPTER 2

MOTIVATION AND SCOPE OF THE THESIS

2.1 Introduction

Organic Light-Emitting Devices provides a comprehensive, wide-ranging and authoritative account of both the science behind OLEDs and of recent developments in the materials used to produce them. It will make a valuable contribution to the research field for chemists, physicists and optical engineers alike. Organic light-emitting diodes (OLEDs), especially phosphorescent OLEDs, have been actively investigated for both display and lighting applications due to their ability to efficiently utilize both singlet and triplet excitons [37]. In particular, white OLEDs have been attractive candidates for future solid state lighting sources since their power efficiencies have surpassed those of incandescent bulbs [38].

Poly (phenylenvinylene) (PPV) as an emission material in polymer light-emitting devices interest in PPV has increased dramatically. As model compounds for the corresponding polymers, oligomers, which have a definite structure and can form a film by thermal evaporation like low-weight molecules, have attracted more and more attention [39-45].

Phosphorescent organic light-emitting diodes (PhOLEDs) based on heavy metal complexes have recently received great attention due to their high internal quantum efficiency, up to 100% of a theoretical value, from contribution of both singlet and triplet excitons for light-emission.[39]. Nonetheless, PhOLEDs have a barrier, to overcome: triplet excitons can diffuse to the adjacent layers due to their long life time, leading to undesired emission or quenching of light. Thus, the confinement of triplet excitons with in an emitting layer (EML) is necessary to deploy phosphorescent emitters, which requires an additional hole-blocking layer (HBL) between an EML and an electron-transporting layer (ETL). The HBL could also be advantageous to control of charge balance by blocking hole-diffusion from the EML into the ETL.

2.2 Motivation

In the year 2002 **Mishra *et al* [40]** investigated that temperature dependence of electroluminescence degradation was in two types of organic light emitting devices (OLEDs) based on tris(8-hydroxyquinoline) aluminum (Alq_3) emitter molecule.

1. without copper phthalocyanine (CuPc).
2. with copper phthalocyanine (CuPc).

Buffer layer at the hole-injecting contact interface. The devices without the CuPc buffer layer demonstrated negligible change in half-life when operated at 22 or 70 °C, while devices with the CuPc layer showed the expected decrease in half-life when the temperature was increased. which identifies Alq_3 cations as unstable, leading to device degradation.

There is another work reported by **Li *et al* [41]** in 2005 prepared the first iridium complexes with a six-membered chelated structure. Similar to the five-member chelated compounds. These complexes show deep red phosphorescent emissions at 650-680 nm with short excited lifetimes of 1.7-3.0s and moderate quantum yields of 0.05-0.11 in deaerated CH_3CN . The decent electroluminescent performance of these species demonstrates their promising feature in OLED displays.

In the same year **Zhang *et al* [42]** who successfully synthesized a new Ir(III) complex, $\text{Ir}(\text{MDPP})_2(\text{acac})$. This complex has good electrophosphorescent emitter in organic light emitting device. The device emits yellow light with a external quantum efficiency of 6.02% and a luminance efficiency of 9.89 lm W^{-1} .

In the year 2006 **Zhang *et al* [43]** synthesized and characterized three diphenylquinoline based iridium complexes. These complexes show strong orange emission, which can be tuned by the introduction of fluorinated substituent on the ligand frame. A highly efficient OLED using complex $\text{Ir}(2\text{-FDPQ})(\text{acac})$ as the dopant has been preliminary demonstrated.

There is another important work reported by **Chen *et al* [44]** in 2007 prepared One-dichloro bridged diiridium complex and three mononuclear iridium (III) complexes based on the 1,3,4-oxadiazole derivatives as cyclometalated ligands and acetylacetonate (acac)

as ancillary ligand have been synthesized. In this paper Lianqing Chen report the new mononuclear iridium complexes. The thermal, photophysical, and electroluminescent properties of these complexes were also studied and investigated their crystal structures, focusing on the thermal, photophysical, and electroluminescent properties of these complexes were also studied.

In the recent year another work reported by **Ulbricht *et al* [45]** In order to incorporate iridium(III) complexes covalently into an oxetane bearing hole transporting matrix, a new oxetane equipped acetoacetate derivative was introduced as an ancillary ligand. Model complexes with an analogical non polymerizable ligand were also prepared in order to perform comparative investigations. Therefore, a series of biscyclometalated Ir(III) complexes, showing orange and green emission were synthesized and fully characterized. The emission maxima are 569 nm for the orange and 518 nm for the green-emitting Ir(III) complexes.

In the year 2009 **Lee *et al* [46]** synthesized a new iridium based complexes containing the bulky przl ligands, exhibit a high luminous efficiency, and thus a good device performance, owing to the bulkiness of the przl ancillary ligands.

In the year 2009 **Ge *et al* [47]** synthesizes phosphorescent iridium (III) diazine complexes emitting yellow or green colors. Steric influence of substituent group or symmetry of the ligand plays a very important role in the cyclometalated procedure. Secondly, the iridium pyrimidine complexes show a significantly blue-shift of the emission band, compared with iridium pyrazine complexes. The iridium pyrazine complex emits yellow light with a maximum peak at 575 nm, whereas the iridium pyrimidine complex emits green light with a maximum peak at 527 nm.

2.3 Scope of the thesis

Use of these phosphorescent Iridium complexes in OLED devices has received considerable attention because of their high phosphorescence quantum efficiency, which is due to mixing the singlet and triplet excited states via spin-orbital coupling and enhancing the triplet state subsequently. 1,3,4-Oxadiazole derivatives are one of the most widely studied classes of electron injection/hole-blocking materials due to their electron

deficiency, high photoluminescence, quantum yield, good thermal and chemical stabilities.

Therefore the aim of this work is focused on

1. Design and synthesis of phosphorescent metal complexes of iridium metal using 1,3,4-oxadiazole as primary ligand and various substituted diketones as secondary ligand.
2. To study the photoluminescence.
3. To employ the mononuclear complexes for the device fabrication as they exhibit much better luminescent properties than the dimer
4. To use these metal complexes as emissive materials in organic light emitting devices.

CHAPTER-3

EXPERIMENTAL

Material synthesis, their characterization and device fabrication

3.1 Synthesis

The two materials have been synthesized. These materials are [Ir(PBD)₂(Thenoyltrifluoroacetylacetonate)] and [Ir(PBD)₂(2,2,6,6-tetramethyl 3,5-heptadione)]. Their synthesis process is explained in subsequent subsections.

3.1.1 Synthesis of Tetrakis[2,5-bis(4-methoxyphenyl)-1,3,4-oxadiazolyl-C²,N] (μ-dichloro)diiridium(III)

Iridium trichloride hydrate (50 mg, 0.157 mmol), reacted with 2.5 equiv of 1,3,4-oxadiazole derivatives in a mixture of ethylene glycol monoethyl ether (14 mL) and double distilled water (5 mL). The reaction mixture was then refluxed under N₂ atmosphere for 24 h. The reaction mixture was cooled to room temperature, and the resulting yellow precipitate was filtered by using Wattman paper and washed with ethanol. The sample was dried under vacuum at 100°C for 6-8 hours (**Figure 3.1**).

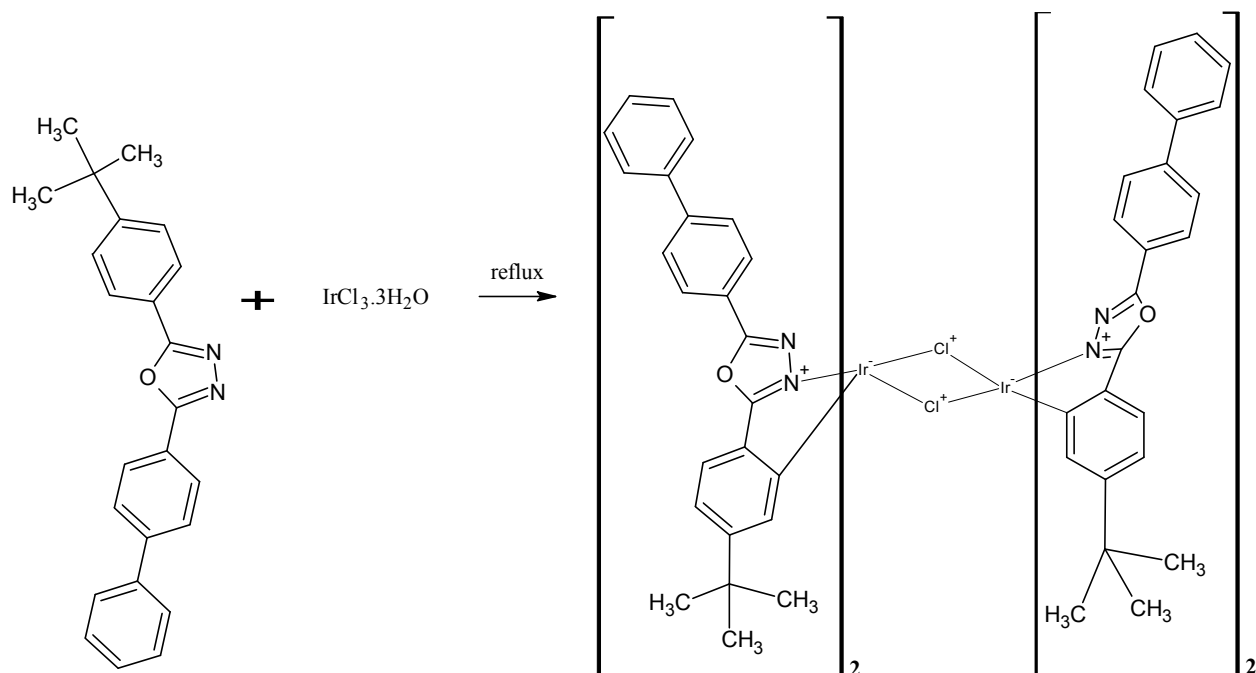


Figure 3.1: Synthesis of Tetrakis[2,5-bis(4 -methoxyphenyl)-1,3,4-oxadiazolyl-C²,N](μ - dichloro)diiridium(III)

3.1.1.1 Synthesis of mononuclear Ir(III) complexes using Thenoyl-trifluoroacetylacetone as secondary ligand.

The dimer (41.5 mg), 149 mmol of secondary ligand, Thenoyltrifluoroacetylacetone, and Na₂CO₃ (63.6 mg) were dissolved in ethylene glycol monoethyl ether (14ml). The mixture was refluxed under N₂ atmosphere for 17-18h. After the sample was cooled to room temperature small quantity of water was added. The resulting yellow precipitate was collected by filtration and washed with ethanol. The sample was dried under vacuum at 100°C for the next 6-8 hours (**Figure 3.2**).

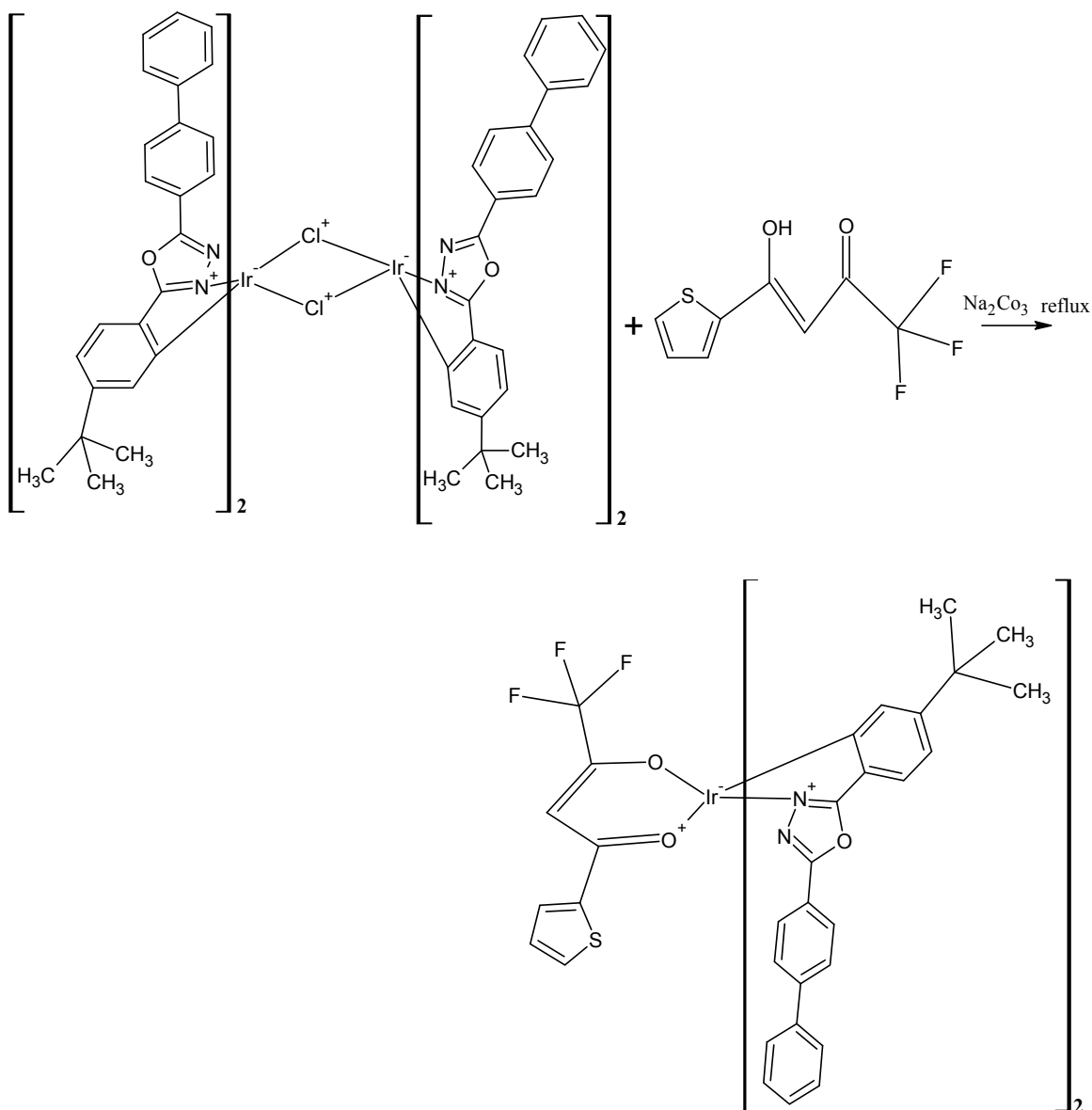


Figure 3.2: Synthesis of mononuclear Ir(III) complexes using Thenoyltrifluoroacetone as secondary ligand

3.1.1.2 Synthesis of mononuclear Ir(III) complexes 2, 2, 6, 6-tetramethyl 3,5-heptadione

The dimer (41.5 mg) and 1ml of secondary ligand, 2, 2, 6, 6-tetramethyl 3,5-heptadione, and Na_2CO_3 (63.6 mg) were dissolved in ethylene glycol monoethyl ether (14 ml). The mixture is refluxed under N_2 for 15-18 h. After the sample is cooled to room temperature small quantity water was added. The resulting yellow precipitate is collected by filtration and washed with ethanol. Then sample was dried under vacuum for 6-8 hour (**Figure 3.3**).

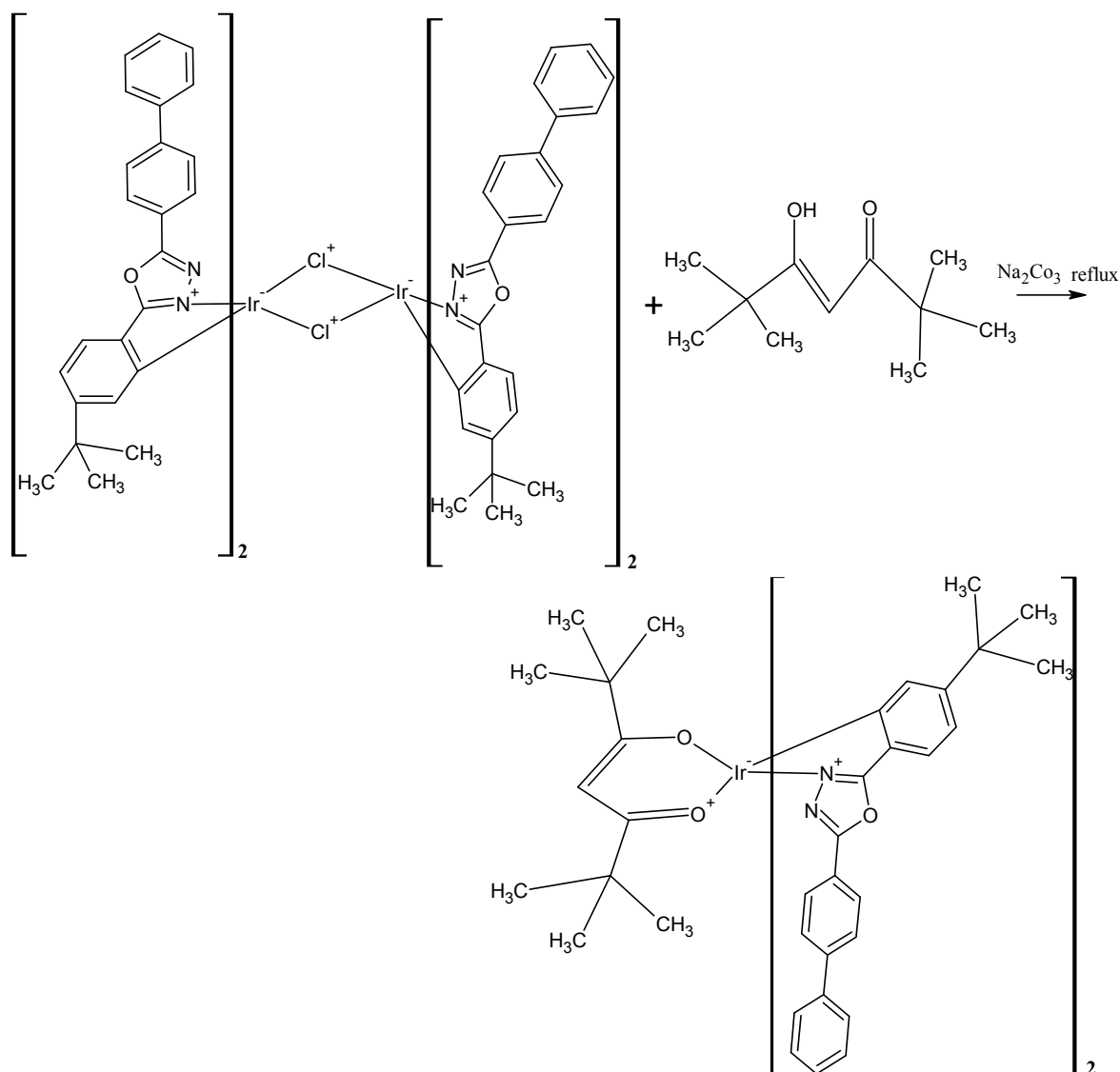


Figure 3.3: Synthesis of mononuclear Ir(III) complexes using 2, 2, 6, 6- tetramethyl 3,5- heptadione as secondary ligand

3.2 Material characterization, device fabrication techniques:

3.2.1 Materials characterization

In material characterization basically we have tried to characterize the synthesized material by variety of techniques to assure that the appropriate materials with suitable properties are synthesized. Some of the characterization techniques used for the characterization of materials is described below.

3.2.1.1 UV- visible spectrometer

UV-visible spectrometer, as illustrated in **Figure 3.4**, is used to determine the optical transmittance of the TCO films. There are four main parts in the spectrometer which are the light source, sample compartment, diode-array detector, and a data acquisition computer. The sample compartment is located between the light source and the detector. The spectrometer measures the amount of ultraviolet and visible light transmitted by a sample which is placed in the sample compartment [48]. In the beginning of the measurement, a pure glass substrate was placed in the sample compartment for the calibration of the spectrometer. After the calibration, the sample, i.e. TCO coated substrate, was then placed in the compartment for the optical transmittance measurement. The principle of UV/Vis measurement is illustrated in **Figure 3.5**. By measuring the initial and the final light intensity I_0 and I , the transmittance ($T = I/I_0$) and absorbance ($A = -\log I/I_0$) of the sample substrate can be determined. The absorbance coefficient α can be calculated according to the equation ($I = I_0 e^{-\alpha t}$)



Figure 3.4: UV- Vis Spectrometer

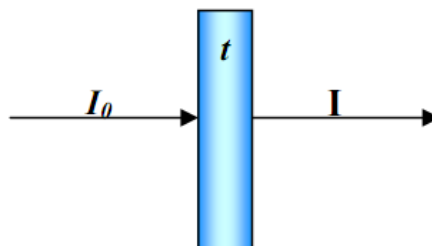


Figure 3.5: Working principle of UV-Vis spectrometry

3.2.1.2 Photoluminescence spectroscopy

Materials structures are investigated using the technique of photoluminescence (PL). A laser is used to photo-excite electrons in material and when they spontaneously de-excite they emit luminescence. The luminescence is analyzed with a spectrometer and the peaks in the spectra represent a direct measure of the energy levels in the semiconductor [49]. The diagram of the photoluminescence spectrophotometer is shown below (Figure 3.6).

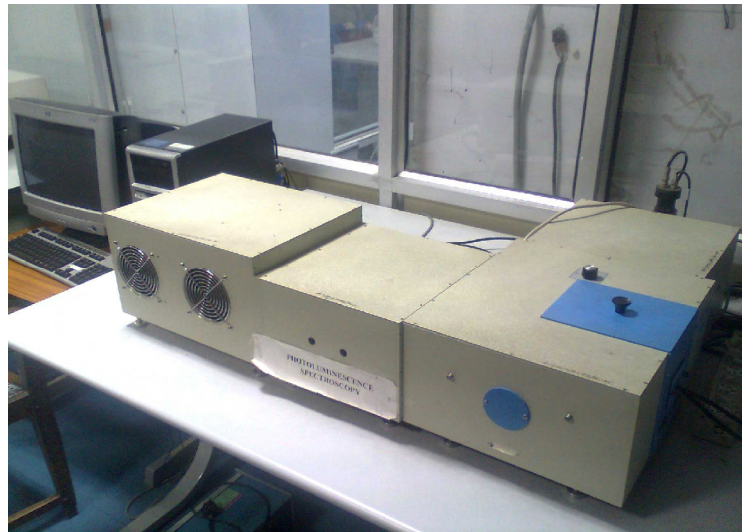


Figure.3.6: Photoluminescence spectrophotometer

All material have so-called “energy gaps” for the conducting electrons. In order to understand the concept of a gap in energy, first consider that some of the electrons in material are not firmly attached to the atoms, as they are for single atoms, but can hop from one atom to another. These loosely attached electrons are bound in the solid by differing amounts and thus have much different energy. Electrons having energies above a certain value are referred to as conduction electrons, while electrons having energies below a certain value are referred to as valence electrons [50]. This is shown in the diagram where they are labeled as conduction and valence bands. The word band is used because the electrons have a multiplicity of energies in either band. Furthermore, there is an energy gap between the conduction and valence electron states. Under normal conditions electrons are forbidden to have energies between the valence and conduction bands. If a light particle (photon) has energy greater than the band gap energy, then it can be absorbed and thereby raise an electron from the valence band up to the conduction band across the forbidden energy gap. (See **Figure 3.7**) In this process of photo excitation, the

electron generally has excess energy which it loses before coming to rest at the lowest energy in the conduction band. At this point the electron eventually falls back down to the valence band. As it falls down, the energy it loses is converted back into a luminescent photon which is emitted from the material. Thus the energy of the emitted photon is a direct measure of the band gap energy, E_g . The process of photon excitation followed by photon emission is called photoluminescence.

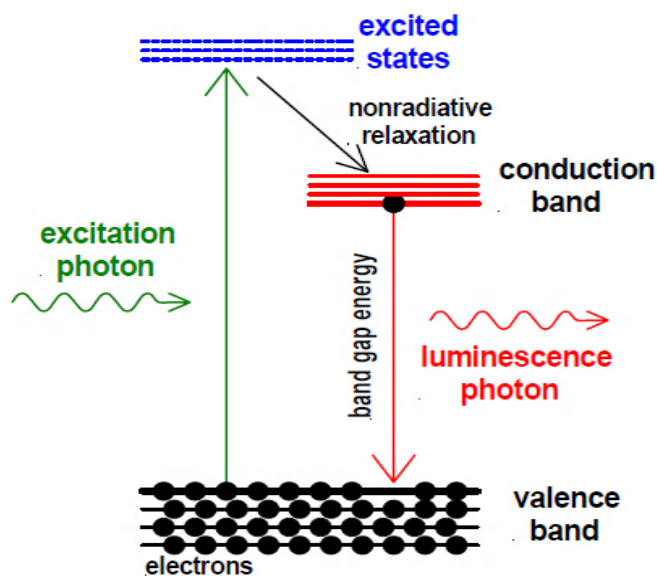


Figure 3.7: Schematic diagram of luminescence.[63]

3.2.1.3 Fourier Transforms Infra-Red spectroscopy.

A molecule absorbs the radiation only when the natural frequency of vibration of some part of molecule (i.e atoms or group of atom comprising it) is the same as the frequency of the incident radiation. After absorbing the correct wavelength of the radiation, the molecule vibrates at increased amplitude. This occurs at the expense of the energy of the IR radiation, which has been absorbed.

Infrared spectroscopy is one of the most powerful analytical techniques, which offer the possibility over the other usual method of structural analysis (X- ray diffraction, electron spin resonance, etc) is that it provides useful information about the structure of the molecule and bonding quickly, without too some evaluation method. Moreover FT-IR provides a very faster of identifying chemical structure especially those of the organic ones.

FT-IR spectroscopy employs an interferometer in place of monochromatic (Figure 3.8). This device generates the Fourier Transform of the infra red spectrum, which is converted to spectrum itself by a computer. This approach has the advantages of providing much higher source radiation throughput, increased signal to noise (S/N) ratio and higher wave number accuracy than is possible with a conventional light dispersive spectrometer [51].

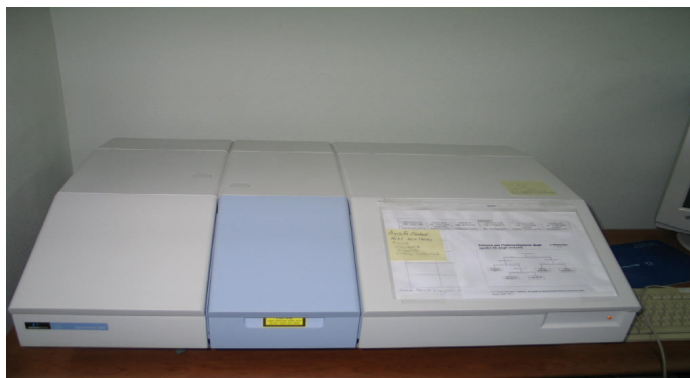


Figure.3.8: FT-IR Spectrophotometer

The technique is based upon the simple fact that a chemical substance shows marked selective absorption in infra red region giving rise to close packed absorption band, called an IR absorption spectrum, which may extend over a wide wavelength range. Various bands in an IR spectrum correspond to characteristic functional groups and bands present in the chemical substance. IR spectrum of a chemical substance is thus a finger print for its identification band position in infrared spectrum may be expressed conveniently by wave number ν , whose unit is cm^{-1} . The relation between velocity c , wavelength λ and frequency ν is as follows:

$$\nu = c / \lambda \quad \text{or} \quad \nu / \text{Cm}^{-1} = \lambda$$

band intensities in IR spectrum may be expressed either as transmittance(T) or absorbance(A). Transmittance is defined as the ratio of the radiant power transmitted by a sample to the radiant power incident on the sample in most spectrum transmittance (T) versus wave number (cm^{-1}) has been plotted.

3.2.1.4 Nuclear magnetic resonance spectroscopy

Nuclear Magnetic Resonance (NMR) is a powerful non-selective analytical tool that enables you to ascertain molecular structure including relative configuration, relative and absolute concentrations, and even intermolecular interactions without the destruction of the analyze. Chemists, with little knowledge of NMR, are now able to obtain 2- or even 3-dimensional spectra with a few clicks of a button. A basic understanding of a few key aspects of NMR spectroscopy can ensure that you obtain the best results possible. This guide is intended to highlight the most pertinent aspects of practical NMR spectroscopy. Nuclei with an odd mass or odd atomic number have "nuclear spin" (in a similar fashion to the spin of electrons). This includes ^1H and ^{13}C (but **not** ^{12}C). The spins of nuclei are sufficiently different that NMR experiments can be sensitive for only one particular isotope of one particular element [52]. The NMR behavior of ^1H and ^{13}C nuclei has been exploited by organic chemist since they provide valuable information that can be used to deduce the structure of organic compounds. These will be the focus of our attention. Since a nucleus is a charged particle in motion, it will develop a magnetic field. ^1H and ^{13}C have nuclear spins of 1/2 and so they behave in a similar fashion to a simple, tiny bar magnet. In the absence of a magnetic field, these are randomly oriented but when a field is applied they line up parallel to the applied field, either spin aligned or spin opposed [53]. The more highly populated state is the lower energy spin state spin aligned situation.

The basic arrangement of an NMR spectrometer is shown below (**Figure 3.9**). The sample is positioned in the magnetic field and excited via pulsations in the radio frequency input circuit. The realigned magnetic fields induce a radio signal in the output circuit which is used to generate the output signal [54]. Fourier analysis of the complex output produces the actual spectrum. The pulse is repeated as many times as necessary to allow the signals to be identified from the background noise.

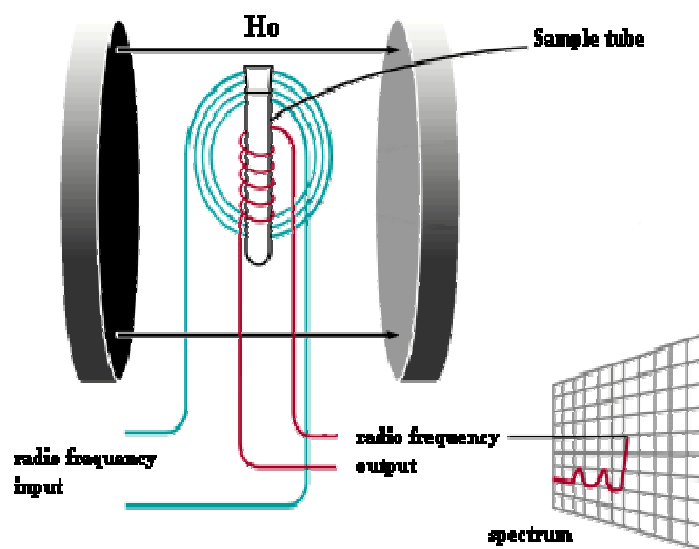


Figure 3.9: Arrangement of NMR spectrometer.[64]

3.2.2 Device fabrication technique:

OLED fabrication includes the deposition of the thin film like. Polymer and metal complexes over a glass substrate which is already coated with Indium Tin Oxide (ITO) which is the anode and a low work function metal is the cathode. Typically organic layer thickness is nearly 100 nm. The term thin film is generally applied to layers that have thicknesses on the order of several micrometers or less. These films may be as thin as a few atomic layers. In many cases, adding atoms or molecules to a substrate surface one at a time forms thin films. The layer whose size is greater than 100 nm called coating. Many technique are used for device fabrication, one of them we used for device fabrication was vacuum evaporation technique. Before preparing a device its patterning is very important. To obtain desired patterns from OLEDs the layer of ITO on glass surface is shaped in a certain manner. It is achieved by Photolithography.

3.2.2.1 Vacuum evaporation technique:

When a pan of water is left to boil on the stove, droplets of water form on the ceiling of the kitchen. If the boiling water is then transferred to a bowl and quickly placed in the freezer, a layer of ice forms above the bowl. Given a high enough temperature, the same cycle of evaporation and condensation can be used to form films of virtually any material that remains stable in a vapor state. When used to apply very thin films in a high vacuum

environment, this process is known as thermal evaporation. This method use high temperature to melt or sublime the target (source material) into vapor state. The atom or molecule of target is speed up by high temperature. Passing through a vacuum space, condensing of a vaporized form to substrate surfaces [55]. The vacuum is required to allow the molecules to evaporate freely in the chamber, and they subsequently condense on substrate surfaces. As the term "Thermal" indicated, the thermal high temperature is the key role of this method. "Thermal High Temperature" is same for all evaporation technologies; only the techniques used to the heat (evaporate) the target differs. Several techniques are used as the thermal high temperature means.

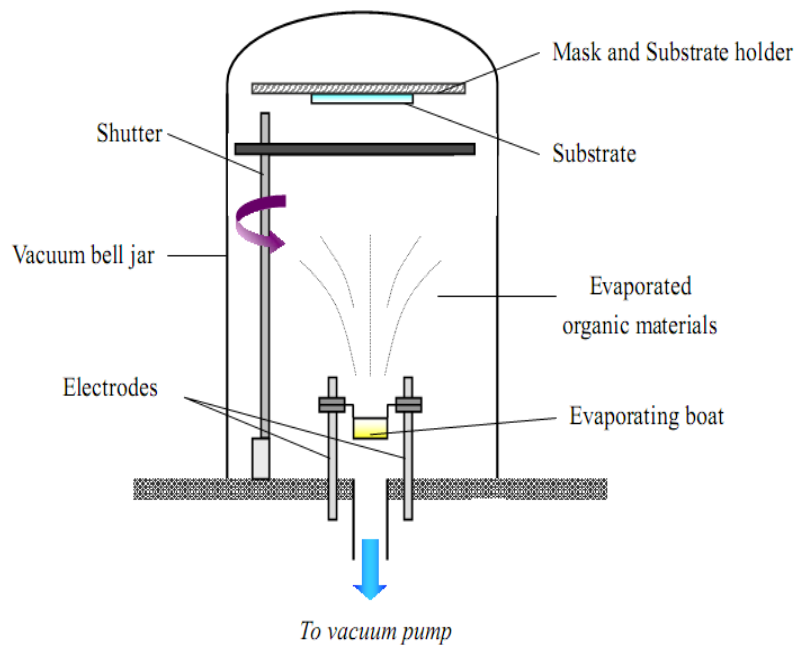


Figure.3.10: Schematic diagram of the thermal vacuum evaporation process.[65]

The vacuum thermal evaporation deposition technique consists in heating until evaporation of the material to be deposited. The material vapor finally condenses in form of thin film on the cold substrate surface and on the vacuum chamber walls (**Figure 3.10**). Usually low pressures are used, about 10^{-6} or 10^{-5} Torr, to avoid reaction between the vapor and atmosphere. At these low pressures, the mean free path of vapor atoms is the same order as the vacuum chamber dimensions, so these particles travel in straight lines from the evaporation source towards the substrate. This originates 'shadowing' phenomenon with 3D objects, especially in those regions not directly accessible from the

evaporation source (crucible). Besides, in thermal evaporation techniques the average energy of vapor atoms reaching the substrate surface is generally low (order of kT , i.e. tenths of eV). This affects seriously the morphology of the films, often resulting in a porous and little adherent material.

3.3 Device fabrication

3.3.1 $\text{Ir(PBD)}_2(\text{Thenoyltrifluoroacetylacetonate})$ and $\text{Ir(PBD)}_2(2,2,6,6\text{-tetramethyl 3,5-heptadione})$ based organic light emitting diode:

The OLED device was fabricated in a configuration ITO/ α -NPD (30nm)/ $\text{Ir(PBD)}_2(\text{Thenoyltrifluoroacetylacetonate})(35\text{nm})$ or $\text{Ir(PBD)}_2(2,2,6,6\text{-tetramethyl 3,5 heptadione})(35\text{nm})/\text{BCP}(6\text{nm})/\text{Alq}_3(28\text{nm})/\text{LiF}(1\text{nm})/\text{Al}$ (as shown in schematic diagram of OLED Device (**Figure 3.11**)). Indium-tin oxide (ITO) coated glass substrates with sheet resistance of $20 \Omega/\square$ were patterned using photolithography and cleaned using dichloroethylene, acetone, isopropyl alcohol and deionised water sequentially for 20 minutes using an ultrasonic bath and dried in flowing nitrogen. Prior to film deposition, the ITO substrates were treated with oxygen plasma for 5 minute. On the substrate, the hole transport layer and the emitting layers were deposited sequentially under a high vacuum (1×10^{-5} torr) at a deposition rate of 0.2 - 0.5 Å/sec and LiF at 0.1-0.2 Å/sec. Thickness of the deposited layers were controlled by a quartz crystal monitor. The cathode was deposited on the top of the structure through a shadow mask. A 30 nm N,Ndiphenyl-N'N'-bis(1-naphthyl)-1,1'-biphenyl-4,4'-diamine(α -NPD) (Sigma Aldrich) was used as hole transport layer. $\text{Ir(PBD)}_2(\text{Thenoyltrifluoroacetylacetonate})$ or $\text{Ir(PBD)}_2(2,2,6,6\text{-tetramethyl 3,5 heptadione})$ was used as the emitting layer and aluminium tris-8-hydroxyquinoline(Alq_3) (Sigma Aldrich) was used as electron transport layer. The electron injection was facilitated using a 1nm thin LiF (Merck, Germany) layer followed by a thick layer of aluminium. The size of each pixel was $4 \times 4 \text{ mm}^2$. The current–voltage (I-V) characteristics were measured using (Keithley 2400).

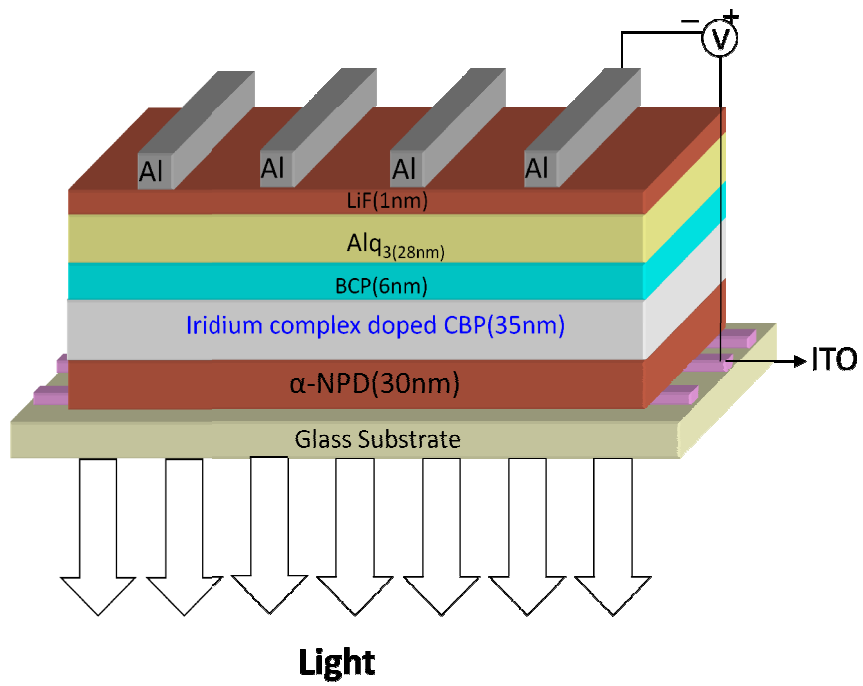


Figure 3.11: Device structure of OLED

CHAPTER 4

RESULTS AND DISCUSSION

4.1 Structural characterization

The structural characterization of these iridium complexes is done by the infrared absorption spectrum in KBr pellets has been studied using a Perkin-elmer (aspectrum BX) spectrometer and by NMR spectrum in CDCl_3 solvent.

4.1.1 Structural characterization of $\text{Ir}(\text{PBD})_2(\text{Thenoyltrifluoroacetylacetonate})$:

The FTIR spectrum and NMR spectrum shown below (**Figure 4.1 & 4.2**) carried out by sample preparation by pellets containing $\text{Ir}(\text{PBD})_2(\text{Thenoyltrifluoroacetylacetonate})$ power (0.1 wt %) dispersed in the KBr power. The spectrum shows the characteristics peak of aromatic ring stretching at 1484 cm^{-1} due to existence of biphenyl ring. The observed peak at 1006 cm^{-1} indicates the presence of C-F stretching. The important peak is observed at 680 cm^{-1} for C-S stretching. The peak at 1314 cm^{-1} is the peak of C-N stretching. Peak at 1074 cm^{-1} shows the C-O stretching. Aromatic C-H stretching is at 3086 cm^{-1} . Presence of C-C is indicated by the peak at 1067 cm^{-1} in the observed spectrum. CHN (calculated: C% 60.04, H% 4.14, N% 5.00; found: C% 59.68, H% 4.17, N% 4.87). The ^1H NMR chemical shifts in complex **2** are found to be as follows: 8.209 (AH); 8.170 (BH); 7.761(CH); 7.655(DH); 7.508(EH); 7.472(FH); 7.416(GH); 1.255(JH) and in thiol 7.327(AH); 7.116(BH).

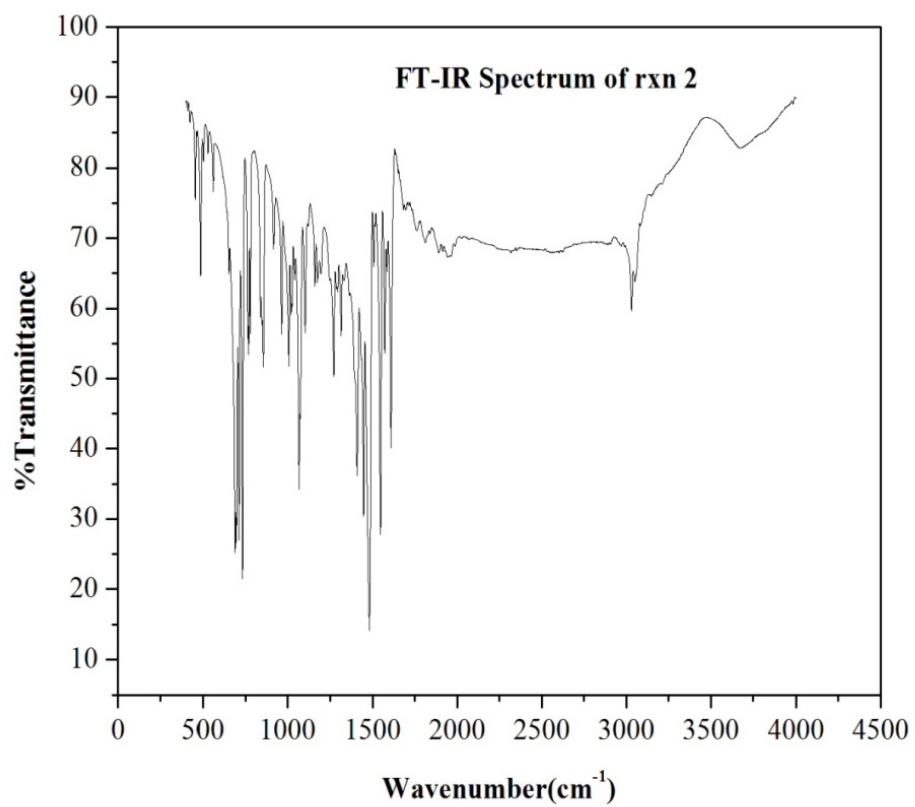
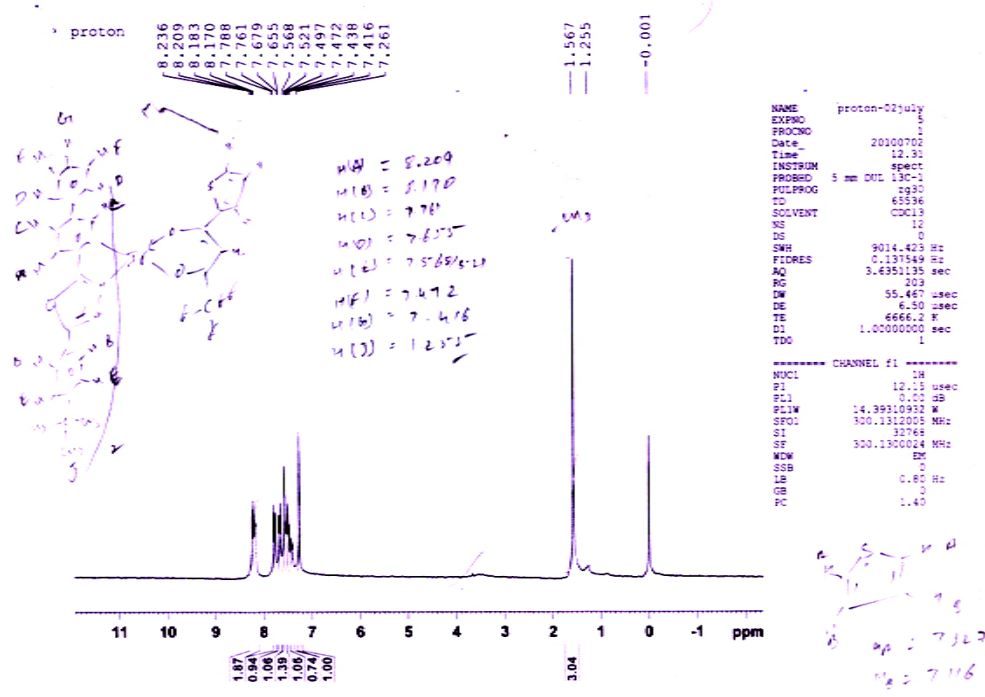
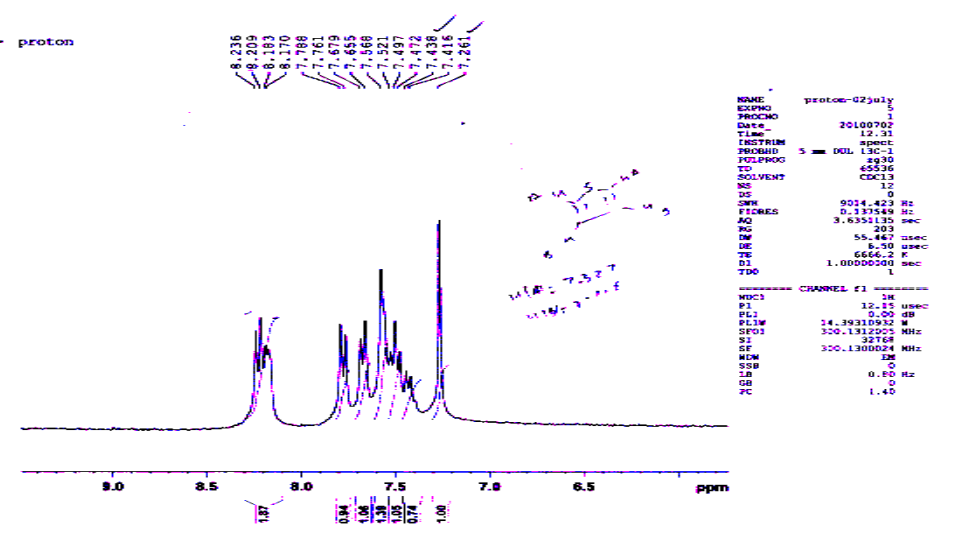


Figure 4.1: FT-IR Spectrum of Ir(PBD)₂(Thenoyltrifluoroacetylacetonate)



(a)



(b)

Figure.4.2: (a) NMR (b) resolved NMR spectra of (PBD)₂(Thenoyltrifluoroacetone) in CDCl₃

4.1.2 Structural characterization of Ir(PBD)₂(2,2,6,6- tetramethyl 3, 5-heptadione):

The FTIR spectrum shown below (**Figure 4.3**) carried out by sample preparation by pellets containing Ir (PBD)₂(2,2,6,6- tetramethyl 3,5-heptadione) power (0.1 wt%) dispersed in the KBr power. The spectrum shows the characteristics peak of aromatic ring stretching at 1610 cm⁻¹ due to existence of biphenyl ring, the peak at 1315 cm⁻¹ is the peak of C-N stretching. Peak at 107cm⁻¹ shows the C-O stretching. Aromatic C-H stretching is at 3086 cm⁻¹. Presence of C-C is indicated by the peak at 1067 cm⁻¹ in the observed spectrum. CHN (calculated: C% 65.47, H% 5.69, N% 5.18; found: C% 65.82, H% 4.04, N% 4.49). The ¹HNMR chemical shift in complex **4** are found to be 8.209 (AH); 8.183(BH); 7.761(CH); 7.655(DH); 7.569(EH); 7.492(FH); 7.415(GH); 1.253(JH).(**figure 4.4**).

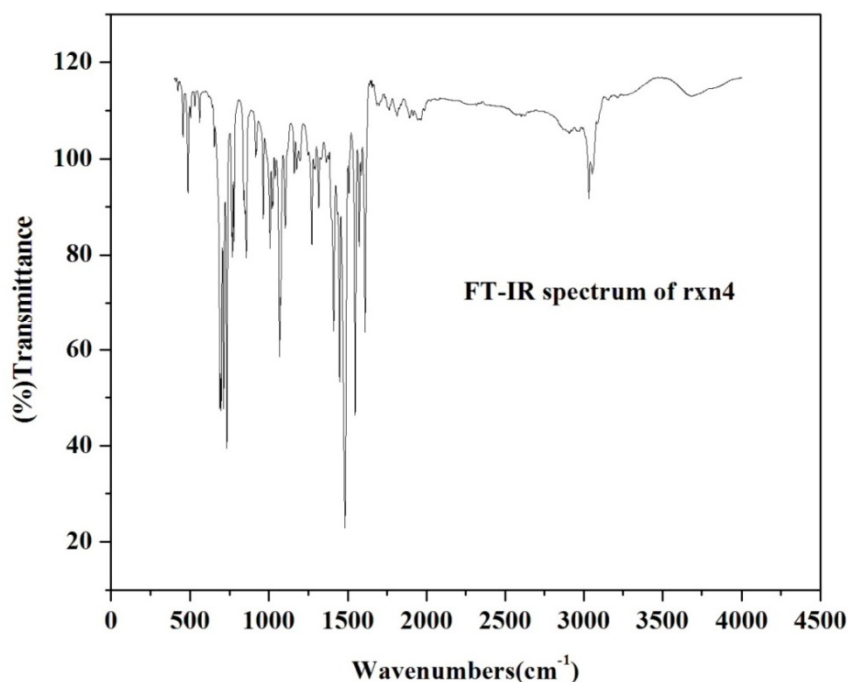
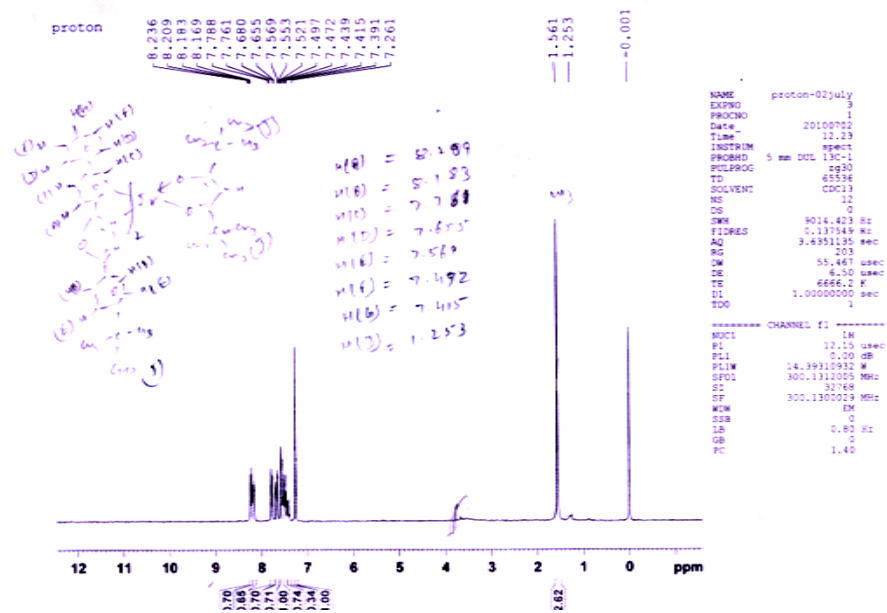
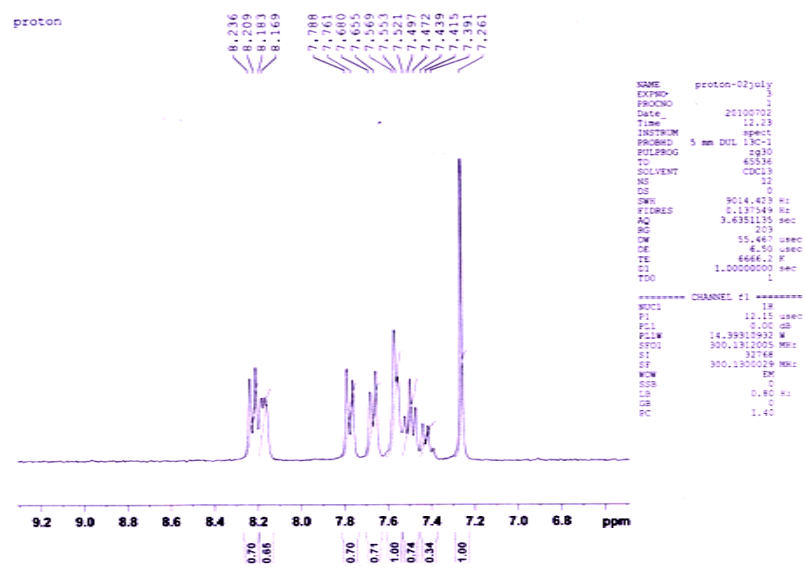


Figure 4.3: FT-IR Spectrum of Ir (PBD)₂(2, 2, 6, 6- tetramethyl 3, 5-heptadione)



(a)



(b)

Figure.4.4 :(a) NMR (b) resolved NMR spectra of the Ir(PBD)₂(2, 2, 6, 6 tetramethyl3,5-heptadione) in CDCl₃

4.2 Optical characterization

UV-visible absorption spectra were recorded on a Shimadzu UV-2401 spectrophotometer. The excitation and emission spectra of a solution of Ir complexes (Horiba Jobin YVON Fluolog Model FL 3-11) at room temperature.

4.2.1 Optical characterization of Ir(PBD)₂(Thenoyltrifluoroacetylacetonate)

The UV-Vis absorption and photoluminescence spectrum were obtained in a solution form with CH₂Cl₂ solvent of Ir(PBD)₂(Thenoyltrifluoroacetylacetonate) and are shown in (Figure 4.5 & 4.6). The intense absorption at 370 nm can be easily assigned to the spin allowed $\pi - \pi^*$ transitions from primary ligand and relatively weaker absorption at 433 nm, ascribing to a spin allowed metal-to-ligand charge transfer (¹MLCT) transition. In comparison to complex 4 it is hypsochromic shift. Beyond 433 nm the long tail extended to lower energies can be likely associated with both ³MLCT and ³ $\pi - \pi^*$ transition. The peak of the PL spectrum of Ir(PBD)₂(Thenoyltrifluoroacetylacetonate) was observed at longer wavelength i.e 559 nm which shows the bathochromic shift.

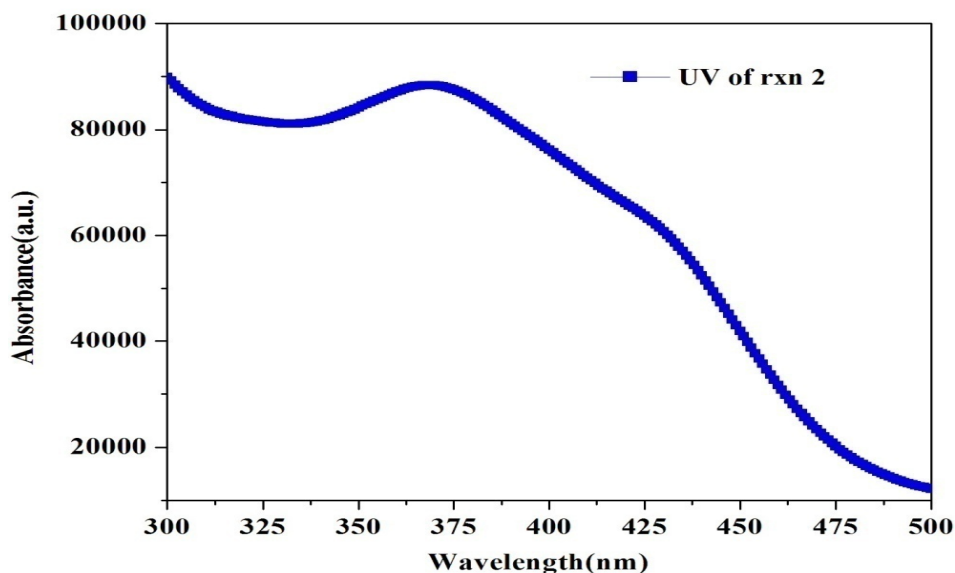


Figure 4.5: Absorption spectra of Ir(PBD)₂(Thenoyltrifluoroacetylacetonate) complexes in CH₂Cl₂ solution

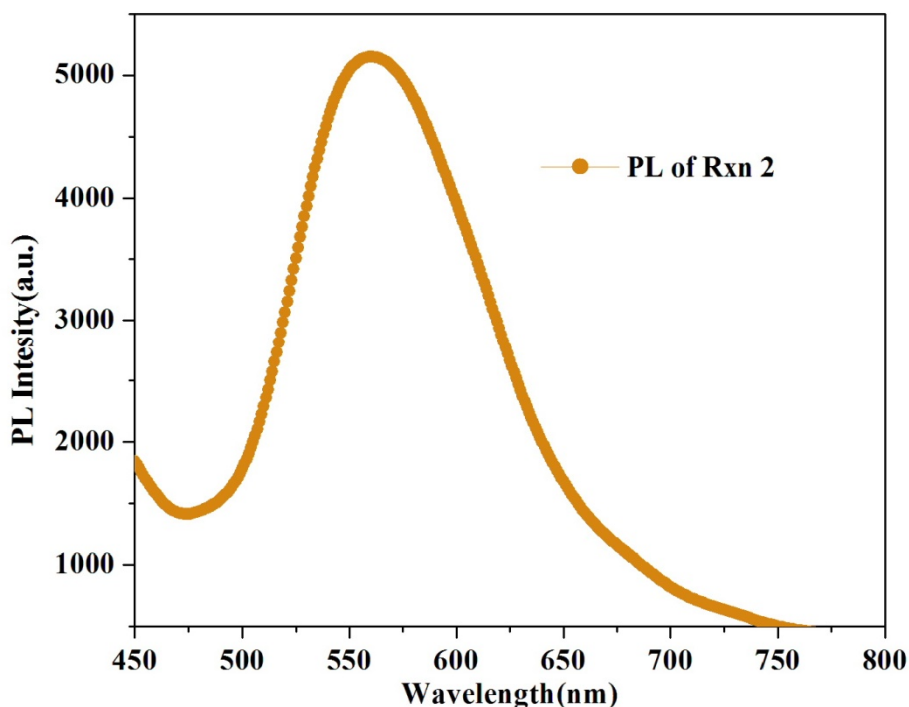


Figure 4.6: PL spectra of Ir(PBD)₂(Thenoyltrifluoroacetylacetonate) in CH₂Cl₂ solution

4.2.2 Optical characterization of Ir(PBD)₂(2,2,6,6-tetramethyl 3,5-heptadione)

The UV-Vis absorption and photoluminescence spectrum were obtained in a solution form of Ir(PBD)₂(2,2,6,6-tetramethyl 3,5-heptadione) and are shown in (**Figure 4.7 & 4.8**). The intense absorption at 362 nm can be easily assigned to the spin allowed π - π^* transitions from primary ligand and relatively weaker absorption at 441 nm, ascribing to a spin-allowed metal-to-ligand charge transfer (¹MLCT) transition. In comparison to complex **2** it is bathochromic shift. Beyond 441 nm the long tail extended to lower energies can be likely associated with both ³MLCT and ³ π - π^* transition. The peak of the PL spectrum of Ir(PBD)₂(2,2,6,6-tetramethyl 3,5-heptadione) was observed at lower wavelength i.e 549 nm which shows the hypsochromic shift.

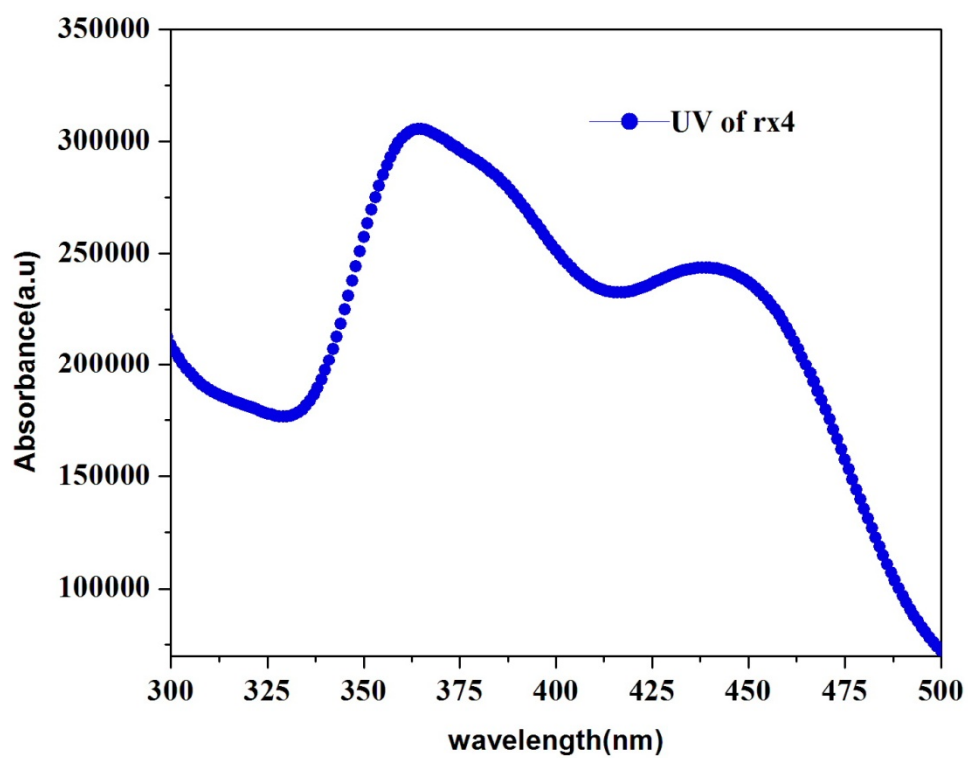


Figure 4.7: Absorption spectra of Ir(PBD)₂(2,2,6,6- tetramethyl 3, 5-heptadione) complexes in CH₂Cl₂ solution

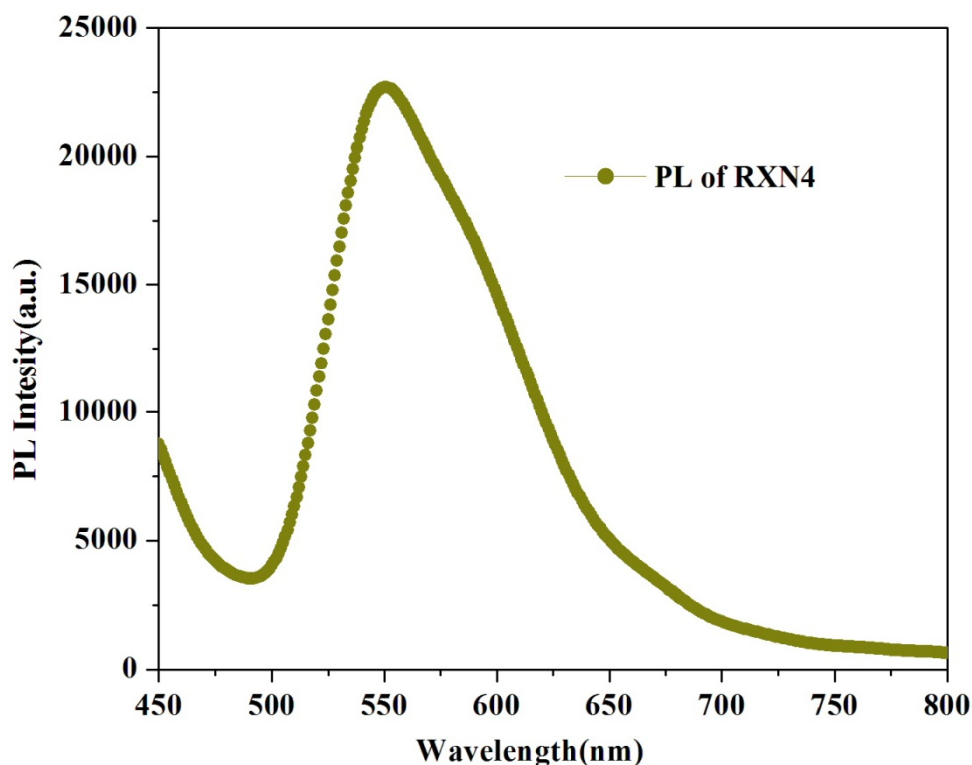


Figure 4.8: PL spectra of Ir(PBD)₂(2,2,6,6-tetramethyl 3, 5-heptadione) in CH₂Cl₂ solution

4.3 Device characterization

The electroluminescent (EL) spectrum which is shown below was taken on a high-resolution spectrometer (HR 2000 CG-UV-NIR). The voltage-current characteristics are measured by using (Keithley 2400).

4.3.1 Device characterization of Ir(PBD)₂(Thenoyltrifluoroacetylacetonate)

The electroluminescence spectra were captured at different applied voltages (**Figure 4.9**). It was observed that the electroluminescence spectrum is similar to photoluminescence, a spectrum which indicates that the EL and PL have the same origin. The EL intensity of the device increases with increase in voltage from 11 V to 12 V, and the peak position remain unchanged 559 nm.

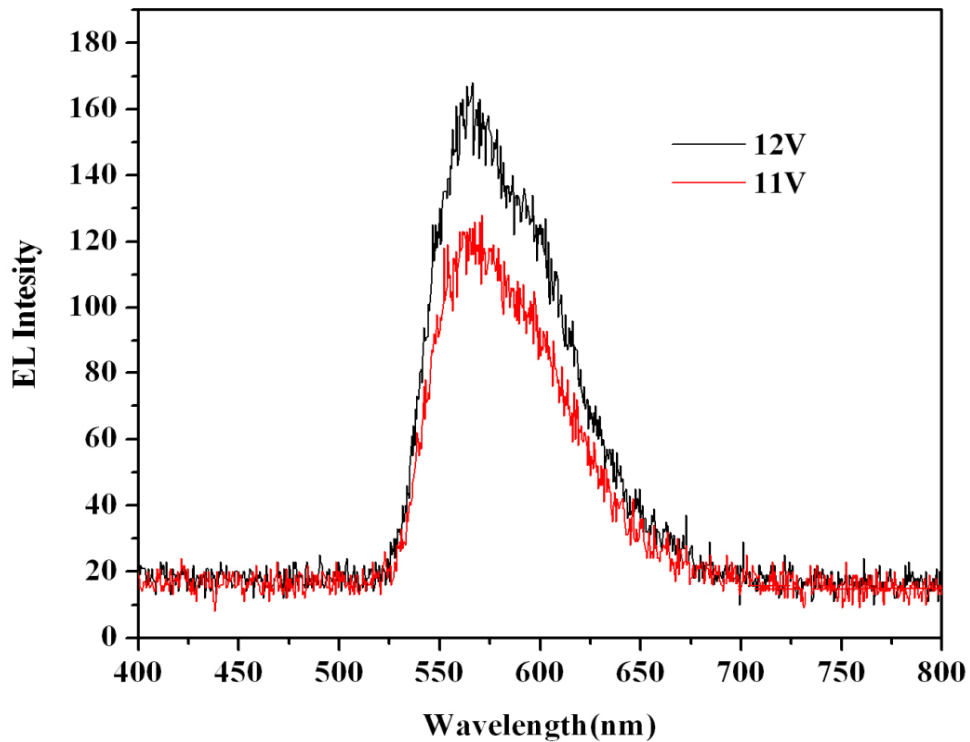


Figure.4.9 : Electroluminescence spectra at different voltages

The current voltage (I-V) characteristic of the fabricated device was captured by applying voltage across the device with ITO as an anode and Aluminium as cathode (forward bias) as shown in (**Figure 4.10**). From the I-V characteristic it has been seen that the onset of light emission starts at about 9V. Above this voltage, the current rises non-linearly due to the space charge effects. Above the threshold voltage the device emits orange yellowish light. Below this voltage the I-V characteristics shows Ohmic current indicating the presence of thermally generated carrier.

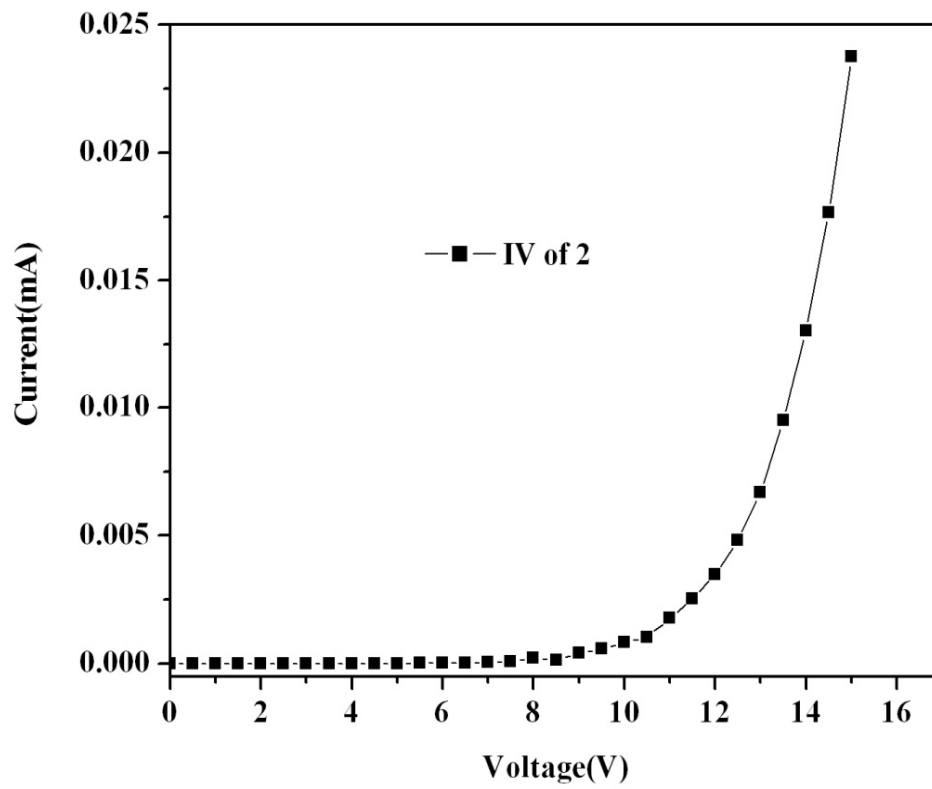


Figure.4.10: I-V characteristics of the device

CHAPTER 5

CONCLUSION AND FUTURE SCOPE

5.1 Conclusion

$\text{Ir(PBD)}_2(\text{Thenoyltrifluoroacetylacetonate})$ and $\text{Ir(PBD)}_2(2,2,6,6\text{-tetramethyl 3,5-heptadione})$ as the novel electroluminescence materials for OLEDs application have been synthesized. The structural characterization of the metal complexes was done by UV-visible absorption spectra, photoluminescence spectra, FT-IR and NMR spectroscopy. The solution of $\text{Ir(PBD)}_2(\text{Thenoyltrifluoroacetylacetonate})$ in CH_2Cl_2 shows intense absorption at 370 nm assigned to spin allowed $\pi\text{-}\pi^*$ transition from primary ligand and relatively weak absorption at 433 nm ascribing to spin allowed metal-to ligand charge transfer ($^1\text{MLCT}$) transition. Beyond 433 nm the long tail extended to lower energies can be likely associated with both $^3\text{MLCT}$ and $^3\pi\text{-}\pi^*$ transition. The photoluminescence peak is at 559 nm and that of $\text{Ir(PBD)}_2(2,2,6,6\text{-tetramethyl 3,5-heptadione})$ shows intense absorption peak at 362 nm assigned to spin allowed $\pi\text{-}\pi^*$ transition from primary ligand and the weaker absorption at 441 nm ascribing to spin allowed metal-to-ligand charge transfer ($^1\text{MLCT}$) transition. Beyond 441 nm the long tail extended to lower energies can be likely associated with both $^3\text{MLCT}$ and $^3\pi\text{-}\pi^*$ transition. The photoluminescence peak is at 549 nm. The OLED device have been fabricated with the structure ITO/ $\alpha\text{-NPD}(30\text{ nm})/\text{Iridium complexes}(35\text{ nm})/\text{BCP}(6\text{ nm})/\text{Alq}_3(28\text{ nm})/\text{LiF}(1\text{ nm})/\text{Al}$, which shows the broad electroluminescence peak.

5.2 Future scope

The work presented in this thesis suggests some further investigations, which may be useful from technological and academic point of view. They are as follows.

1. Searching of some other oxadiazole derivatives having good electron affinities and to study their transport behaviour for better electron injection and charge transportation. Their optical behaviour also need to be studied.
2. Design some ancillary ligand, which can take charge easily from central metal atom (MLCT)

References.

- [1]. C. W. Tang and S. A. VanSlyke, *Appl. Phys. Lett.* **51**, 913 (1987).
- [2]. Y. Divayana and X. W. Sun, *Appl. Phys. Lett.* **90**, 203509 (2007).
- [3]. M. Pope, H. P Kallmann, and P. Magnante, *J. Chem. Phys.* **38**, 2042 (1963).
- [4]. C. Adachi, S. Tokito, T. Tsutsui, and S. Saito, *J. Appl. Phys.* **27**, L269 (1988).
- [5]. J. H. Burroughes, D. D. C. Bradley, A. R. Brown, R. N. Marks, K. Mackay, R. H. Friend, P. L. Burns and A. B. Holmes, *Nature*. **347**, 539 (1990).
- [6]. S. Hotta and K. Waragai, *Adv. Mater.* **5**, 896 (1993).
- [7]. M. A. Baldo, D. F. O'Brein, Y. You, A. Shoustikov, S. Sibley, M. E. Thompson, and S. R. Forest, *Nature*. **395**, 151 (1998).
- [8]. M. M. Beerbom, B. L. agel, A.J. Cascio, B.V. Doran and R. Schlaf, *J. Electron Spectrosc. Relat. Phenom.* **152**, 12 (2006).
- [9]. J. S. Vincett, W. A. Barlow, R. A. Hann, *Thin Solid Films.* **94**, 171 (1982).
- [10]. M. Pope and C. E. Swenberg, *Appl. Phys. Lett.* **70**, 1233 (1997).
- [11]. A.Yeh, M.S Jan and T. R Chen, *Mat. Lett.* **61**, 259 (2007).
- [12]. A. Sharma, D. Singh and J.K. Makrandi. *Mat. Lett.* **61**, 4614 (2007).
- [13]. J. L. Morancais, L. G. H. P. Falzgraf *Transition Met. Chem.* **9**, 130 (1984).
- [14]. J. A. Cheng, C. H. Chen and H. P. D. Shieh, *Mat. Chem. and Phys.* **113**, 1003 (2009).
- [15]. C. Kittel, *Introduction to Solid State Physics* (Wiley & Sons) (1986).
- [16]. R.H. Friend, N.C. Greenham, pp. 823, (1998), *Handbook of Conducting Polymers*, (NewYork: Marcel Dekker Inc.).
- [17]. M. Ikai, S. Tokito, Y. Sakamoto, T. Suzuki and Y. Taga, *Appl. Phys. Lett.* **79**, 156 (2001).
- [18].] J. L. Maldonado, M. Bishop, C. F. Hernandez, P. Caron and M. Malagoli, *Chem. Mat.* **15**, 994 (2003).
- [19]. G. Gustafsson, Y. Cao, G. M. Treacy, F. Klavetter, N. Colaneri, and A. J. Heeger, *Nature*. **357**, 477 (1992).
- [20]. J. Weckesser, J. V. Barth and K.Kern, *J. Chem. Phys.* **110**, 11 (1999).
- [21]. C. B. Murphy, Y. Zhang, T. Troxler, V. Ferry and J.J. Martin, *J. Phys. Chem.* **108**, 1537 (2004).

- [22]. P. W. M. Blom, H. F. M. Schoo and M. Matters, *Appl. Phys. Lett.* **73**, 26 (1998).
- [23]. M. Era, C. Adachi, T. Tsutsui, S. Saito, *Chem. Phys. Lett.* **178**, 488 (1991).
- [24]. S. H. Jeong, B. N. Park, D. G. Yoo and J. H. Boo, *J. Korean Phys. Soc.* **50**, 3 (2007).
- [25]. F. Nuesch, L. J. Rothberg, E. W. Forsythe, Q. T. Le, Y. Gao, *Appl. Phys. Lett.* **74**, 880 (1999).
- [26]. N. Agarwal and P. K. Nayak, *Tetrahed Lett.* **49**, 2710 (2008).
- [27]. W. Brutting, S. Berleb and A. G. Muckl, *Org. Elect.* **2**, 1 (2001).
- [28]. L. H. Smith, J. A. E. Wasey and W. L. Barnes, *Appl. Phys. Lett.* **84**, 16 (2004).
- [29]. Q. T. Le, F. Nuesch and E. W. Forsythe, *Appl. Phys. Lett.* **75**, 1357 (1999).
- [30]. S. D. Wang, W. K. Wong, C. S. Lee and S. T. Lee, *Appl. Phys. Lett.* **79**, 1561 (2001).
- [31]. L. S. Hung, C. W. Tang and M. G. Mason, *Appl. Phys. Lett.* **70**, 152 (1997).
- [32]. <http://www.siliconchip.com.au/>.
- [33]. T. H. Lee, K. L. Tong, S. K. So and L. M. Leung, *Synth. Met.* **155**, 116 (2005).
- [34]. S. C. Chang, J. Bharathan, Y. Yang, R. Helgeson, F. Wudl, M. B. Ramey and J. R. Reynolds, *Appl. Phys. Lett.* **73**, 2561 (1998).
- [35]. *Flat Panel Displays Advanced Organic Materials* by S. M. Kelly, RSC publishing (2000).
- [36]. A. Kohler, J. S. Wilson and R. H. Friend, *Adv. Mater.* **14**, 701 (2002).
- [37]. M. A. Baldo, M. E. Thompson and S. R. Forrest, *Phys. Rev.* **B 60**, 14422 (1999).
- [38]. J. Kovac, L. Peternai and O. Lengyel, *Thin Solid Films.* **433**, 22 (2003).
- [39]. K. Sugiyama, H. Ishii, Y. Ouchi, and K. Seki, *J. Appl. Phys.* **87**, 297 (2000).
- [40]. A. Mishra, P. K. Nayak and N. Periasamy, *Tetrahed. Lett.* **45**, 6265 (2004).
- [41]. H. C. Li, P. Chou and Y. H. Hu, *Org. Mett.* **24**, 1329 (2005).
- [42]. G. Zhang, and Y. Chuai, *Mat. Lett.* **59**, 3002 (2005).
- [43]. X. W. Zhang, C. L. Yang and Z. A. Li, *Chin. Chem. Lett.* **17**, 411 (2006).
- [44]. L. Chen, C. Yang and M. Li, *Crystal Grow. Des.* **7**, 39 (2007).
- [45]. C. Ulbricht, N. Rehman and E. Holder, *Mac. Chem. Phy.* **210**, 531 (2009).
- [46]. H. S. Lee, S. Y. Ahn, J. H. Seo and Y. K. Kim, *J. Korean Phys. Soci.* **55**, 1977 (2009).
- [47]. G. Ge, J. He and H. Guo, *J. Organomet. Chem.* (2009).
- [48]. P. N. M. Anjos and H. Aziz, *Org. Elect.* **39**, 13 (2002).

- [49]. B. W. D. Andrade and S. R. Forrest, *Adv. Matter.* **16**, 1585 (2004).
- [50]. Q. Xu, H. Z. Chen, J. Z. Sun and M. Wang Chin, *Chem. Lett.* **16**,159 (2005).
- [51]. H. T. Lu and M. Yokoyama, *J. Crystal Grow.* **260**, 186 (2004).
- [52]. *Organic Spectroscopy* by Willium Kemp (W.H. Freeman & Company) (1991).
- [53]. *Organic Spectroscopy* by Y.R Sharma (S. Chand & Company) (2005).
- [54]. T. Mori, H. Fujikawa, S. Tokito and Y. Taga, *Appl. Phys. Lett.* **73**, 2763 (1998).
- [55]. I.H. Kazi, P. M. Wild, T. N. Moore and M. Sayer, *Thin Solid Films.* **433**, 337 (2003).
- [56]. web.uvic.ca/ail/techniques/epi-fluorescence.html
- [57]. www.absoluteastronomy.com/topics/Franck-Condon
- [58]. www.cstf.kyushu-u.ac.jp/.../research_a_e.html
- [59]. spectrum.ieee.org
- [60]. spie.org/x23960.xml
- [61]. polymer.hnu.kr/sub/sub02/sub_0201_04.jsp
- [62]. www.fibre2fashion.com/industry-article
- [63]. www.olympusmicro.com/.../fluoroexciteemit.html
- [64]. www.analyticalspectroscopy.net/ap7-2.htm
- [65]. www.ece.utep.edu